The impact of the direct effects of sulfate and black carbon aerosols on the sub-seasonal march of the East Asian subtropical summer monsoon

Dongdong Wang and Bin Zhu, Collaborative Innovation Center on Forecast and Evaluation of Meteorological Disasters, Nanjing University of Information Science & Technology, Nanjing, China

Zhihong Jiang, Key Laboratory of Meteorological Disaster of Ministry of Education, Nanjing University of Information Science & Technology, Nanjing, China

Xiu-Qun Yang, CMA-NJU Joint Laboratory for Climate Prediction Studies, Institute for Climate and Global Change Research, Nanjing University, Nanjing, China.

Tong Zhu, CIRA/Colorado State University, Fort Collins, CO, USA

NOAA/NESDIS/STAR/JCSDA, College Park MD, USA

Corresponding author: Bin Zhu, Collaborative Innovation Center on Forecast and Evaluation of Meteorological Disasters, Nanjing University of Information Science & Technology, Nanjing 210044, China (binzhu@nuist.edu.cn)

Key points

Aerosol direct effects could change the zonal land-sea thermal contrast.

Sulfate and BC have an opposite effects in the middle parts of the troposphere.

Aerosol direct effects change the East Asia subtropical summer monsoon march.

This is the author manuscript accepted for publication and has undergone full peer review but has not been through the copyediting, typesetting, pagination and proofreading process, which may lead to differences between this version and the Version of Record. Please cite this article as doi: 10.1002/2015JD024574

Abstract

Aerosol emissions have rapidly increased in East Asia since the late 1970s. During the same period, the East Asian Summer Monsoon (EASM) has shown a weakening trend. In this work, the direct effects (DE) of sulfate and black carbon (BC) aerosols on the sub-seasonal (pentad mean) march of the East Asian subtropical summer monsoon (EASSM) are investigated using an interactive global climate-chemistry model. The simulation results suggest that the DE of sulfate aerosols have a notable effect on the cooling of the low troposphere across the continent in spring and autumn, hence, changing the time of the seasonal transition of the zonal land-sea thermal contrast (ZTC). The DE of BC result in cooling of the low troposphere and heating of the middle troposphere, leading to a different impact than that caused by sulfates. The cooling of the surface and troposphere by sulfates leads to a delay in the warming of East Asian continent in spring, and the EASSM onset time; it also accelerates the process of the continent turning colder and advances the retreat of the EASSM. The deeper heating in the middle-upper troposphere than the cooling in the low troposphere due to the DE of BC or the combination of both leads to an advance in the onset time of the monsoon caused by the continent turning warmer earlier in spring. In autumn, the same cooling effect by sulfates leads to the continent turning colder earlier, resulting in an advance in the retreat time.

1. Introduction

Monsoon is defined as the tropical and subtropical seasonal reversal in both the surface winds and the associated precipitation, which is caused by differential heating between a continental-scale land mass and the adjacent ocean [*Intergovernmental Panel on Climate Change* (*IPCC)*, 2007]. The East Asian region is one of the largest monsoon regions in the world. The unique location of this region within the continent and ocean causes a large meridional and zonal land-sea thermal contrast between the Asian continent and the western Pacific, leading to a complex and distinct East Asian monsoon system [*Yeh et al.*, 1959; *Tao and Chen*, 1987]. The East Asian summer monsoon (EASM) system can be divided into two independent subsystems: the South China Sea summer monsoon (SCSM) and the East Asian subtropical summer monsoon (EASSM, i.e., the subtropical monsoon covering areas from mainland China to Japan) [*Zhu et al*., 1986; *He et al*., 2008]. Some studies [*He et al*., 2008; *Qi et al*., 2008; *Zhao et al*., 2009] have further distinguished between the mechanisms of the SCSM and EASSM systems; according to these studies, the onset of SCSM depends on the seasonal transition of the meridional land-sea thermal contrast (MTC), while the EASSM relies more on the reversal of the zonal land-sea thermal contrast (ZTC).

The EASM exerts a dominant effect on the summer climate in East Asia, providing about 40-50% of the annual mean precipitation over southern China and about 60-70%

over northern China [*Lei et al.*, 2011; *Song et al.*, 2014]. Some studies found a weakening trend and southward migration of the precipitation zone of EASM beginning in the late 1970s [*Wang*, 2001; *Yu et al*., 2004; *Xu et al*., 2006; *Ding et al*., 2008, 2009; *Zhou et al*., 2009]. The possible mechanisms for the interdecadal change in the EASM is an active research topic [*Zhou et al.*, 2009; *Song et al.*, 2014]. Various factors, such as sea surface temperature (SST) variability [*Xue*, 2001; *Wang*, 2002; *Yang and Lau*, 2004; *Li et al*., 2010a; *Zhou and Zou*, 2010], sensible heat flux over the Tibetan Plateau [*Ding et al*., 2009; *Wu et al*., 2012; *Liu et al*., 2012], anthropogenic forcing (aerosols and greenhouse gases) [*Xu*, 2001; *Menon et al*., 2002; *Ueda et al.*, 2006; *Liu et al.*, 2009; *Li et al*., 2010b; *He et al.*, 2013; *Wang et al.*, 2013; *Song et al.*, 2014; *Zhu et al*., 2012], and natural decadal variability [*Jiang and Wang*, 2005; *Lei et al*., 2011], have been linked to the interdecadal change in the EASM. *Song et al.* [2014] suggested that the internal variability mode of Pacific Decadal Oscillation (PDO) might play a dominant role in the weakening of the monsoon, while aerosol forcing plays a secondary or complementary role.

Over the past several decades, East Asia has witnessed tremendous economic development, causing a dramatic increase in the emissions of aerosols and aerosol precursor gases [*Bond et al.*, 2007; *Lamarque et al*., 2010; *Smith et al.*, 2011], which has been accompanied by one of the most significant environmental issues-air pollution [*Liao et al.*, 2015]. Anthropogenic sulfur dioxide (SO_2, a precursor gas for

sulfate) and BC are two major sources of anthropogenic aerosols over East Asia. The emissions of anthropogenic SO_2 in East Asia in the 2000s were approximately five times greater than that in the 1960s [*Smith et al.,* 2011]. Further, while the anthropogenic BC emissions in East Asia were about 26 Gg $year^{-1}$ in the 1950s, they rose to about 690 Gg $year^{-1}$ in the 2000s [*Bond et al.,* 2007]. Sulfate aerosols, formed from SO_2, and BC aerosols in the atmosphere have led to a large increase in aerosol loading in East Asia [*Lefohn et al*., 1999; *Bond et al*, 2007; *Streets et al*., 2008; *Junker and Liousse,* 2008]. These aerosol emissions can play an important role in climate change.

The DE of aerosols implies the mechanism through which the aerosols directly affect the atmosphere, involving scattering and absorbing solar radiation, thereby altering the radiative balance of the Earth-atmosphere system. Sulfate aerosols scatter and reflect the incident shortwave radiation and thus reduce the amount of shortwave radiation reaching the surface (also called "solar dimming"), decrease surface air temperature, suppress monsoon circulation, and decrease the amount of precipitation over South and East Asia [*Xu,* 2001; *Gu et al.,* 2006; *Huang et al.,* 2007; *Kim et al.,* 2007; *Liu et al.,* 2009; *Cowan and Cai,* 2011; *Zhang et al.,* 2011; *Jiang et al.,* 2013; *Guo et al.,* 2013; *Zhou et al.,* 2014].

Unlike sulfate aerosols, BC aerosols absorb the incoming shortwave radiation,

resulting in cooling of the surface and heating of the atmosphere. However, the BC and sulfate aerosols differ in their effects on the vertical structures of air temperature and atmospheric circulations. Many researchers have analyzed the mechanisms by which BC aerosols affect the monsoon systems over South and East Asia [*Menon et al.*, 2002; *Chung and Zhang*, 2004; *Ramanathan et al.*, 2001, 2005; *Lau et al.*, 2006; *Lau and Kim*, 2006; *Wang*, 2007; *Meehl et al.*, 2008; *Randles and Ramaswamy*, 2008; *Gautam et al.*, 2009; *Ming et al.*, 2010; *Cowan and Cai*, 2011; *Ganguly et al.*, 2012; *Mahmood and Li*, 2011, 2013a, 2013b].

The studies on the radiative effects of aerosols on monsoons have mainly been aimed at the South Asian summer monsoon (SASM) and EASM or the changes in the summer monsoon precipitation, wherein the monsoon is usually discussed in terms of a seasonal average, while the sub-seasonal changes have received much less attention [*Bollasina et al.*, 2013]. However, it is important to understand the sub-seasonal march of a monsoon, especially its onset, as it is critical for agriculture planning and water management [*Zhao et al.*, 2007; *Bollasina et al.*, 2013]. Many researchers have considered the effects of aerosols on the pre-monsoon period, and on the onset of the summer monsoon and precipitation [*Bollasina et al.*, 2008, 2013; *Meehl et al.*, 2008; *Wang et al.*, 2009; *Lau and Kim*, 2010; *Ji et al*., 2011; *Martin et al.*, 2013; *Mahmood and Li*, 2013b]; however, most of these studies were focused on the SASM. Overall, the nature of changes in the monsoon onset is still an under-explored topic, because of

the elusive physical mechanisms associated with it and the complex nature of the onset itself [*Bollasina et al.,* 2013].

From the previous studies, the impact of aerosols on the processes of onset, development, and retreat of the East Asian monsoon, especially the EASSM, has not been clear. *Wang et al*. [2014] focused on the DE of sulfate aerosols on the surface temperature and the seasonal transition of the ZTC in East Asia. In this study, we focus on the different nature of the effects of sulfate and BC aerosols, as well as their combined effects, on the sub-seasonal march of the EASSM. The analysis and simulation are conducted using version 5.1 of the Community Atmosphere Model (CAM5.1). The rest of the paper is structured as follows. The model descriptions and experimental design are given in Section 2. The analysis of the DE of aerosols on the sub-seasonal march of EASSM is given in Section 3. Discussion and conclusions drawn from the study are presented in Sections 4 and 5, respectively.

2. Model and experimental design

In this study, we used a coupled global climate-chemistry model, CAM5.1 [*Neale et al*., 2010] including the chemistry and aerosol mechanism [MOZART, *Emmons et al*., 2010], radiation mechanism [RRTMG, *Iacono et al*., 2008], and microphysical and macroscopic mechanisms associated with clouds [*Morrison and Gettelman*, 2008; *Gettelman et al*., 2010] to evaluate the effects of sulfate and BC aerosols. The

MOZART mechanism has a representation of aerosols based on the work by *Tie et al.* [2001, 2005], i.e., sulfate aerosol is formed by the oxidation of SO_2 in the gas phase (by reaction with the hydroxyl radical) and in the aqueous phase (by reaction with ozone and hydrogen peroxide). Because only the bulk mass is calculated, a lognormal distribution is assumed for all aerosols using a different mean radius and geometric standard deviation [*Liao et al.,* 2003]. Natural aerosols (desert dust and sea salt) are implemented following *Mahowald et al.* [2006a, 2006b]. In addition, secondary organic aerosols (SOA) are linked to the gas-phase chemistry through the oxidation of atmospheric non-methane hydrocarbons (NMHCs), as in *Lack et al.* [2004]. Greenhouse gas forcing was maintained at its present-day (year 2000) value. The sources of aerosol emissions were taken from the emissions inventory of *Emmons et al*. [2010].

Our aim was to explore the DE of sulfate and BC aerosols, both individually and collectively, on the EASSM. The EASM is controlled by the land-sea thermal contrast, and the atmospheric heating over land dominates this contrast [*Jiang et al.*, 2013]. The land-sea contrast in the heating capacities makes the land cool down more readily under aerosol forcing, driving a preferential cooling over land [*Song et al.*, 2014]. As a consequence, the SST responses to the climate system were excluded in this study; and we based our methodology on the experiments conducted under the Atmospheric Model Intercomparison Project (AMIP) to examine the atmosphere-land (fast)

response to aerosol forcing [*Jiang et al.,* 2013, 2015].

Four numerical experiments were conducted with the prescribed monthly mean climatological sea surface temperature (SST) and sea ice in this study, including a control experiment (Ctrl) that included all types of direct and indirect radiative processes of aerosols and three sensitivity experiments (nSO4de, nBCde, and nSO4BCde), as shown in Table 1. In each of the sensitivity experiments, one or two types of DE of aerosols were turned off by setting the aerosol optical depth (AOD) to zero during the calculation of direct radiation, while all the others were preserved. Here, the DE of BC include the direct and semi-direct effects [*Hansen et al.,* 1997; *Ackerman et al.,* 2000]. The experiments without the DE of sulfate aerosols were marked as nSO4de, and those without the DE of BC aerosols were marked as nBCde. The experiments that eliminated the DE of both the sulfate and BC aerosols were marked as nSO4BCde. The differences between the results of the Ctrl and sensitivity experiments were regarded as the DE of aerosols on the climate. While our sensitivity experiments highlight the DE of aerosols to extreme levels, they do not represent the real situation. A 2-year low-pass filter was applied to suppress the interannual variability and a t-test was used to assess the significance of these differences.

The CAM5.1 model uses the MOZART chemistry mechanism with a horizontal resolution of 1.9° latitude and 2.5° longitude, and 30 vertical levels. Each experiment

was run for 31 years, but only the last 30 years of the simulations were used in our study. In addition, the 2.5° × 2.5° daily meteorological variables from the National Centers for Environmental Prediction/National Center for Atmospheric Research (NCEP/NCAR) reanalysis [*Kalnay et al.*, 1996] database were used to validate the simulated atmospheric circulation.

3. Results

3.1. Aerosol direct radiative effects

The aerosol concentrations are distributed mainly over the East Asian continent and its adjacent oceans. Figure 1 shows the time-latitude cross section of AOD for the sulfate and BC aerosols and the total precipitation rate and meridional wind at 850 hPa for the longitude range of 105°-120°E from the Ctrl experiment. As shown in Fig. 1a, during winter and early spring, the sulfate AOD is distributed in the 20°-35°N range, and the highest values of AOD are concentrated in the 25°-30°N range. Starting around the 21st pentad, the lowering in the AOD values is caused by the precipitation during the pre-flood season in southern China (Fig. 1b) [*Zhu et al.*, 2011]. The area with high AOD values decreases and moves toward northern China (35°-40°N) in summer. Then, the high-AOD area moves northward because of the effect of the dominant low-level south airflow in the EASM, as shown in Fig. 1b, which is consistent with the results of *Jiang et al.* [2015].

Sulfate aerosols as secondary pollutants experience more active conversion from SO_2 gas to particulate sulfate in summer because of higher solar radiation and stronger photochemical reactions [*Guo et al.,* 2013; *Liao et al.,* 2015]. In spite of the strong wet scavenging process, the greater amount of water vapor that enhances the hygroscopic growth of sulfate aerosols also likely results in the higher AOD value in summer. In autumn, the relatively higher solar radiation and weaker wet scavenging processes also result in high AOD values, and then, the area with high AOD values moves southward because of the transition of wind fields (Fig. 1b).

The AOD values for the simulated BC aerosols are distributed mainly at latitudes of 20°-40°N (Fig. 1a), with the high AOD values being distributed in the 25°-35°N range depending on the emission levels. However, the annual cycle of the north-to-south movement of BC AOD is not obvious compared to the movement of sulfate AOD (Fig. 1a). This is because BC aerosols, which act as primary pollutants, have relatively stable physical and chemical characteristics and are less susceptible to transport by wind fields and to wet scavenging, compared to SO_2 gas (precursor of sulfate aerosols) [*Guo et al.,* 2013]. The AOD of BC reaches its maximum value in winter and spring, while it reaches its minimum in summer because of wet scavenging and the intruding air masses from the clean ocean [*Jiang et al.,* 2015].

The maximum average of BC is only approximately 0.03, which is much less than that of sulfate aerosols (Fig. 1a). It should be noted that the aerosol forcing efficiency of the BC aerosols (-220 $W \cdot m^{-2} \cdot \tau^{-1}$; τ is AOD) is much higher than that of the sulfate aerosols (-30 $W \cdot m^{-2} \cdot \tau^{-1}$), indicating that BC aerosols can produce greater radiative forcing on the climate per unit AOD [*Conant et al.*, 2003; *Schulz et al.*, 2006]. As such, the DE of both BC and sulfates are important to the East Asian climate.

The DE of aerosols lead to the scattering and absorption of solar flux, and alter the thermal structure of the atmosphere. The DE of both sulfate and BC aerosols result in less solar radiation reaching the surface under clear-sky conditions, thus resulting in a negative change in the net solar flux at the surface (Fig. 2). The distribution of the change in the net solar flux caused by the DE of aerosols at the surface under clear-sky conditions is consistent with the values of AOD (Fig. 1), which is consistent with the results of *Jiang et al.* [2015]. The long wave flux change under clear-sky conditions by the DE of aerosols is found to be small (figure not shown).

3.2. Change in air temperature by the DE of aerosols

The changes in surface air temperature induced by the DE of sulfate, BC, and the combination of both are shown in Fig. 3. The DE of sulfate (Fig. 2a) lead to negative radiative forcing at the surface under clear-sky conditions for almost the entire year, as well as a decrease in the surface air temperature (Fig. 3a), in most of the

continental areas in China (20°-50°N, 105°-120°E). However, the change in surface air temperature does not correspond to the change in net solar flux at the surface under clear-sky conditions (Fig. 2) because of the cloud feedback [*Jiang et al.*, 2015]. With the movement of the EASM, low-level south airflow prevails over East Asia (Fig. 1b), which transports sulfate aerosols northward, and consequently, the clear-sky net solar radiative forcing at the surface also moves northward (Fig. 2a). In this study, the only difference between the Ctrl and sensitive experiments were the aerosol direct effects. The change in surface air temperature is dominated by the change in the solar flux induced by the DE of aerosols and the feedback from the changes in the clouds. As a result, the centers of decreased surface air temperature move northward to the north of 30°N in summer, then move back to 20°N in autumn in accordance with the movement of negative radiative forcing (Fig. 3c).

The DE of BC aerosols also result in negative radiative forcing; however, the changes are small, as shown in Fig. 2b. The changes in surface air temperature are small and most of the values are not statistically significant (Fig. 3b), which may be caused by the semi-direct effects partially counteracting the DE of BC [*Guo et al.*, 2013; *Jiang et al.*, 2013, 2015]. The DE from the combination of sulfate and BC aerosols (Fig. 2c) are similar to those from sulfates individually. A few differences exist between the DE of the two types of aerosols in terms of the surface air temperature in winter, and both are insignificant. From spring to autumn, the changes

in surface air temperature are mainly driven by the DE of sulfates (compare Fig. 3c with 3a).

In this study, the key region is the East Asian subtropical continent (27.5°-32.5°N, 105°-120°E) [*He et al*., 2008; *Qi et al*., 2008; *Zhao et al*., 2009]. Figure 4 shows the time-altitude cross section of air temperature changes induced by the DE of sulfates, BC, and a combination of both sulfates and BC over the subtropical continent (27.5°-32.5°N, 105°-120°E). Both sulfate and BC aerosols play a role in cooling the surface; however, the upper-middle troposphere responds to sulfate and BC aerosols in an opposite manner [*Liu et al.,* 2009; *Jiang et al.,* 2013]. Sulfate aerosols scatter solar radiation and thus lead to atmospheric cooling, whereas BC aerosols absorb solar radiation and thus lead to atmospheric heating.

Generally, the diabatic heating of the atmosphere includes shortwave heating (QRS), longwave heating (QRL), heating from vertical diffusion (DTV), and condensational heating from moisture processes (DTCOND) [*Jiang et al.*, 2013]. The QRS change due to aerosols is a result of BC absorption of shortwave flux. The change in QRL is a result of the change in cloud and water vapor. The DTV change is a result of vertical heat transfer from the surface. The change in DTCOND is a result of the latent heat release by deep convection [*Liu et al.,* 2004]. The DTCOND contribute to the Asian summer monsoon formation and dominate diabatic heating

over East Asia [*Jin et al.*, 2013]. Figure 5 shows the time-altitude cross section of QRS, DTCOND, and vertical velocity changes induced by the DE of sulfates, BC, and a combination of both sulfates and BC over the subtropical continent.

In Fig. 4a, the air temperature over the subtropical continent is reduced below 850 hPa and increased above 850 hPa in winter because of the DE of sulfates. In early spring and autumn, a significant decrease in air temperature at both the surface and troposphere is caused by the DE of sulfates. Additionally, a significant reduction in air temperature in the middle-upper troposphere occurs in autumn, mainly contributed by the reduced DTCOND in keeping with the weakened ascending motion owing to the change in circulation (Fig. 5b). In summer, the air temperature is reduced below 850 hPa and increased above 850 hPa because of sulfates; however, the increase is not significant (Fig. 4a).

The increase in air temperature caused by the DE of BC (Fig. 4b) occurs almost throughout the entire year, except in early spring (below 700 hPa) and autumn (insignificant decrease). The increase in air temperature is partly contributed by the increase in the shortwave heating rate (QRS, Fig. 5c) because of the absorption of BC and the increase in DTCOND in accordance with the enhanced ascending motion resulting from the change in circulation (Fig. 5d). As shown in Fig. 5c, the concentrations of BC and QRS are maintained below 500 hPa in winter, which then

move to the upper troposphere in early spring and fall back below 500 hPa in autumn because of atmospheric circulation.

The DE of the combination of sulfates and BC aerosols (Fig. 4c) cause an increase in the air temperature in winter. In early spring, a significant cooling of the low troposphere (below 700 hPa) and warming of the middle-upper troposphere (above 700 hPa) occurs, and the increase in air temperature is partly contributed by the increase in the QRS (Fig. 5c) resulting from the absorption of BC. In summer, the air temperature falls below 850 hPa and increases above 850 hPa. In contrast, in autumn, a significant reduction in the air temperature occurs near the surface and in the middle-upper troposphere in autumn; this result is similar to that for sulfates. However, the DE of the combination of two types of aerosols is not a linear summation [*Liu et al.*, 2009; *Jiang et al.*, 2013].

As discussed above, the surface cooling in spring is caused by the DE of aerosols resulting from decreased solar radiation reaching the surface (Fig. 2), and the middle-upper troposphere heating (Fig. 4) is partly contributed by the increase in the QRS (Fig. 5) because of the absorption of BC. This mechanism is consistent with the results of the previous work [*Gu et al.*, 2006; *Huang et al.*, 2007; *Meehl et al.*, 2008; *Liu et al.*, 2009; *Ming et al.*, 2010; *Jiang et al.*, 2013; *Guo et al.*, 2013]. In autumn, the surface cooling is also mainly driven by the DE of aerosols (Fig. 2); however, the

reduction of air temperature in the middle-upper troposphere is mainly caused by the decrease in DTCOND in accord with the weakened ascending motion resulting from the change in circulation (Fig. 5). Most of the change in QRL (figure not shown) is negative, and partly offsets the change in QRS. The negative DTV (figure not shown) results in a cool lower troposphere because of the decreased surface air temperature due to aerosol direct effects (Fig. 2 and Fig. 3). The response of DTCOND is a feedback of the DE of aerosols [*Jiang et al.,* 2013]. As a result, the DE of aerosols make an important contribution toward the change in tropospheric air temperature over the East Asian subtropical continent in spring and autumn, which are also the key periods for the onset and retreat of the EASSM.

3.3. Aerosol direct effects on the zonal land-sea thermal contrast

The land-sea thermal contrast is generally considered to be the fundamental mechanism of monsoon formation. The ZTC is the key driving force of the EASSM, and the quickest rise in temperature and lowering in air pressure occurs at the latitude of 30°N, where the seasonal cycle of ZTC first transits [*He et al*., 2008; *Qi et al*., 2008; *Zhao et al*., 2009]. Aerosol direct effects bring about negative surface radiative forcing and result in a decrease in the surface temperature, hence changing the land-sea thermal contrast [*Liu et al.,* 2009; *Zhang et al*., 2011; *Jiang et al*., 2013]. In

addition, the contrast in the land-sea heating capacities and the often higher aerosol loading over land make the land cooler than the ocean under aerosol forcing.

Temperature latitudinal deviation (TLD) is defined as the discrepancy between the temperature at a given longitude and the mean temperature averaged over 105°-150°E at some selected latitudes. Figure 6 shows the temporal evolution of TLD at 850 hPa and 500 hPa at the latitude of 30°N from the Ctrl experiment and the NCEP/NCAR reanalysis data. The simulated temporal evolution of TLD at 850 hPa and 500 hPa at the latitude of 30°N is consistent with the NCEP/NCAR reanalysis. As shown in Fig. 6, the west Pacific is warm in winter, turns cool in early spring, being located east of 130ºE, then turns warm again in autumn. In contrast, the Asian continent is cold in winter, becomes warm in early spring, being located west of 120ºE, then turns cold again in early autumn. As a result, the East Asia continent is defined in terms of its location at 105º-120ºE and the west Pacific is defined as 130º-150ºE. In comparison to the other global climate models, CAM5.1 captures the characteristics of the temporal evolution of TLD well [*Jiang et al.*, 2013, 2015].

As discussed in Fig. 6, the ZTC is defined as the temperature difference between the western Pacific Ocean (130°-150°E) and the East Asian continent (105°-120°E), where the most significant subtropical area is the region located at the latitude of 30°N [*He et al*., 2008; *Qi et al*., 2008; *Zhao et al*., 2009]. Figure 7a shows the

temporal evolution of the ZTC at 850 hPa at a latitude of 30°N from the simulation experiments. From the results of the Ctrl experiment (Table 2), the transition times of the ZTC are found to be around the 16th and 55th pentad. In the sensitivity experiments, the transition times of the ZTC are around the 15th and 56th pentad in the nSO4de experiment, the 15th and 55th pentad in the nBCde experiment, and the 14th and 56th pentad in the nSO4BCde experiment at 850 hPa. Adopting the spatial test method, similar to *Song and Zhou* [2014], the change in timing of the ZTC is significant.

Figure 8 shows the time-longitude cross section of the changes in air temperature at 850 hPa by DE along the 30°N latitude. In accord with Fig. 4, the DE of sulfates and the combination of sulfates and BC decrease the air temperature from early spring to autumn over the East Asian continent (105°-120°E) at 850 hPa (Fig. 8a, c). The decrease in air temperature is significant in spring and autumn. However, the decrease in air temperature by the DE of BC is small and insignificant (Fig. 8b). By comparing the Ctrl experiment with sensitivity experiments, it was found that low troposphere cooling by DE of aerosols leads to colder air temperatures across the East Asian continent in spring and autumn, thus the East Asian continent turns warmer later in spring and colder earlier in autumn. As a result, the DE of aerosols lead to the first transition time of the ZTC at 850 hPa being later in spring, and the second transition time being earlier (except BC) in autumn, as shown in Table 2.

As shown in Fig. 7b, the transition times of the ZTC are around the 15th and 55th pentad in the Ctrl experiment at 500 hPa. In the sensitivity experiments, the transition times of the ZTC are around the 15th and 55th pentad in the nSO4de experiment, the 16th and 55th pentad in the nBCde experiment, and the 16th and 55th pentad in the nSO4BCde experiment at 500 hPa. However, according to the Ctrl experiment, the DE of BC and the DE of the combination of sulfates and BC cause the first transition time of the ZTC to be earlier at 500 hPa.

Figure 9 shows the time-longitude cross section of the changes in air temperature at 500 hPa by DE along the 30°N latitude. The DE of sulfate decrease the air temperature in spring and autumn over the East Asian continent (105°-120°E) at 500 hPa (Fig. 9a). The DE of BC and the DE of the combination of sulfates and BC increase the air temperature in spring and decrease the air temperature in autumn (Fig. 9b, c). A comparison of the Ctrl experiment with the sensitivity experiments shows that the air temperature at 500 hPa becomes warmer in spring and colder in autumn over the East Asian continent because of the DE of BC and the DE of the combination of sulfates and BC. The continent turns warmer earlier in spring and turns colder earlier in autumn. As a result, the DE of BC and the DE of the combination of sulfate and BC lead to the first transition time of the ZTC at 500 hPa being earlier in spring, as shown in Table 2.

3.4. Aerosol direct effects on the sub-seasonal march of EASSM

It is well-known that the fundamental features of a typical monsoon domain are a seasonal variation in the low-level winds, especially in wind directions, and distinct alternation between wet and dry seasons. Thus, defining onset dates of the summer monsoon based on wind and/or rainfall is useful for studying the seasonal march of the summer monsoon [*Zhao et al.*, 2007]. Based on the thermal-wind equation, the decrease or increase in the zonal temperature gradient may lead to a decrease or an increase, respectively, in the vertical shear of the geostrophic meridional wind between the upper and lower layers of the troposphere [*Zhao et al.*, 2007]. Generally, the vertical difference in the meridional wind between 200 hPa and 850 hPa is used to represent the thermal wind. As aerosols are mainly distributed in the mid-low level of the troposphere, the direct impacts on the changes in the meridional wind at 200 hPa are small (only 1 pentad later in the first transitions by the DE of BC; figure not shown). Therefore, the change in the thermal wind may be represented as the change in meridional wind at 850 hPa.

As shown in previous works, EASSM is a monsoon system that differs from a tropical monsoon, in that the onset and retreat times depend on the establishment of the transition of the ZTC [*Zhao et al*., 2007; *He et al*., 2008; *Qi et al*., 2008]. Therefore, the establishment criterion for EASSM is the transition of northerly winds

into southerly winds in the subtropics (27.5°-32.5°N, 110°-140°E) at 850 hPa. The criteria for EASSM used in this study are similar to those used by *He et al*. [2008] and *Wang et al*. [2014]: (a) the onset pentad of meridional wind turns positive ($V_{850} > 0$ m s^{-1}); (b) V_{850} remains positive in the subsequent four pentads (including the onset pentad), or at least three pentads, and the mean of four accumulative pentads of meridional wind is greater than 0.5 m s^{-1} ($V_{850} \geq 0.5$ m s^{-1}); (c) the retreat pentad is defined as the time when the meridional wind turns negative ($V_{850} < 0$ m s^{-1}).

Based on the above criteria, the temporal evolution of the meridional wind averaged over the subtropics (27.5°-32.5°N, 110°-140°E) at 850 hPa in the simulation experiments are shown in Fig. 10 and Table 2. The EASSM onset and retreat time for the Ctrl experiment are around the 18th and 56th pentad, respectively. In the sensitivity experiments, the EASSM onset and retreat times are around the 17th and 57th pentad in the nSO4de experiment, the 19th and 57th pentad in the nBCde experiment, and the 19th and 58th pentad in the nSO4BCde experiment. Compared with the Ctrl experiment, the DE of sulfate lead to a 1 pentad delay in the onset and a 1 pentad advance in the retreat time of EASSM. The DE of BC cause a 1 pentad advance in both the onset and retreat time. The DE of the combination of sulfate and BC lead to a 1 pentad advance in the onset and 2 pentads advance in the retreat time of EASSM.

4. Discussion

Previous studies have reported the severe increase in emissions of aerosols and aerosol precursor gases over the past several decades, especially from the second half of the 20th century [*Bond et al.*, 2007; *Lamarque et al.*, 2010; *Smith et al.*, 2011]. Based on the NCEP/NCAR reanalysis, the seasonal march of EASSM from 1950 to 2009 found in this study changes obviously. Figure 11 shows the onset and retreat time of EASSM from 1950 to 2009 based on our EASSM criteria and the total SO_2 emissions estimated for every decade in China. The correlation coefficients of the trend of EASSM onset and retreat have a statistical significance above the 95% level. As shown in Fig. 11, the averaged onset and retreat time of EASSM is around the 18th and 55th pentad from 1950 to 2009. The onset time is delayed and the retreat time is advanced around 1980. In the same period, a dramatic increase in total SO_2 emissions (Fig. 11) as well as BC emissions [*Bond et al.*, 2007] appears. Accordingly, we divide this period (1950-2009) into 1950-1979 (BF1980) and 1980-2009 (AF1980). Figure 12 shows the ZTC of the two periods at 850 hPa and 500 hPa. In AF1980, the first reversal time of the ZTC at both 850 hPa and 500 hPa are later than in BF1980, while the second reversal time is earlier. Based on the results of simulation, the DE of sulfate may be one of the contributors to the changes of EASSM. However, the changes in the march of the monsoon are complex [*Bollasina*

et al., 2013]. There also various factors linked to the changes, such as SST variability. The determination of the detailed mechanism requires further study.

Some limitations of the study should be acknowledged. First, in this study, we focus on the aerosol effects on the march of EASSM; in order to highlight the DE of aerosols on the changes in the air temperature over East Asia, we exclude the internal variation of SST and the responses of SST to the climate system. In addition, *Guo et al.* [2013] indicated that the change in SST caused by aerosols is not significantly greater than the internal variation of SST. Second, the feedback of DE cannot be excluded, which adjusts the atmospheric circulation, thus resulting in changes in the clouds and radiation. Third, the aerosols considered in this study only include sulfate and BC, which are the likely major contributors to the aerosol effect in East Asia. However, other aerosols such as organic carbon (OC), nitrate aerosols, and dust aerosols also exist. In addition to the effects of these aerosols, the effects on cloud and precipitation (indirect effects) will also be studied in the future.

5. Conclusions

In this study, the direct effects (DE) of sulfate and BC aerosols on the sub-seasonal (pentad mean) march of the East Asian subtropical summer monsoon (EASSM) are investigated using a global climate-chemistry model, version 5.1, of the Community Atmosphere Model (CAM5.1). The EASSM is mainly driven by the ZTC between the

East Asian region and the western North Pacific. The onset and retreat time of EASSM depend on the establishment of the transition of the ZTC [*Zhao et al*., 2007; *He et al*., 2008; *Qi et al*., 2008]. Based on previous studies, we use an establishment criterion of EASSM as the transition of northerly winds into southerly winds in the subtropics (27.5°-32.5°N, 110°-140°E) at 850 hPa.

Unlike previous studies on the seasonal average of monsoons, we focus on the different effects of sulfate and BC aerosols on the sub-seasonal march of EASSM. Our results suggest that the aerosol optical depth (AOD) of sulfate is distributed mainly in East Asia and its adjacent oceans. The DE of sulfate on the cooling of the surface and troposphere over the East Asian subtropical region are significant, especially in spring and autumn. At 850 hPa, the cooling by the DE of sulfate result in East Asia turning warmer later in spring and turning colder earlier in autumn, as well as, delaying/advancing the first/second reversal time of the ZTC. As a result, the change in the ZTC by the DE of sulfate likely leads to the delay and advance of the onset time and retreat time, respectively, of EASSM. The distribution of AOD of BC is similar to that of sulfate, but the DE of BC decrease the air temperature of the low troposphere and increase the air temperature of the middle-upper troposphere over the East Asian subtropical region.

The DE of the combination of sulfate and BC significantly decrease the air

temperature of the low troposphere in early spring and autumn over the East Asian subtropical region, mainly because of the DE of sulfate, and significantly increases the middle-upper troposphere air temperature in early spring, mainly because of the DE of BC. As a result, the significant decrease in the low troposphere air temperature leads to the region turning warm later in spring and turning cold earlier in autumn; however, the significant greater increase in the air temperature of the middle-upper troposphere in early spring leads to the region turning warm earlier. Consequently, the change in the ZTC caused by the DE of the combination of sulfate and BC likely results in the advance of the onset and retreat time of EASSM. Moreover, the effect of the combination of two types of aerosols is not a simple linear summation.

Acknowledgments. We would like to thank Dr. E. Kalnay for providing the NCEP/NCAR reanalysis data. This work was supported by grants from the National Basic Research Program of China (grant no. 2010CB428505), the National Natural Science Foundation of China (grant no. 41275143), and the Natural Science Foundation of the Higher Education Institutions of Jiangsu Province, China (12KJA170003). The NCEP/NCAR reanalysis data are available at http://www.esrl.noaa.gov/psd/data/gridded/data.ncep.reanalysis.html.

References

Ackerman A. S., O. B. Toon, D. E. Stevens, A. J. Heymsfield, V. Ramanathan, and E.

J. Welton (2000), Reduction of tropical cloudiness by soot. Science 288, 1042-1047, doi:10.1126/science.288.5468.1042.

Bollasina, M. A., Y. Ming, and V. Ramaswamy (2013), Earlier onset of the Indian monsoon in the late twentieth century: The role of anthropogenic aerosols, Geophys. Res. Lett., 40, 3715-3720, doi:10.1002/grl.50719.

Bollasina, M., S. Nigam, and K.-M. Lau (2008), Absorbing aerosols and summer monsoon evolution over South Asia: An observational portrayal, J. Clim., 21, 3221-3239, doi:10.1175/2007JCLI2094.1.

Bond, T. C., E. Bhardwaj, R. Dong, R. Jogani, S. Jung, C. Roden, D. G. Streets, and N. M. Trautmann (2007), Historical emissions of black and organic carbon aerosol from energy-related combustion, 1850-2000, Global Biogeochem. Cycles, 21, GB2018, doi:10.1029/2006GB002840.

Chung, C. E., and G. J. Zhang (2004), Impact of absorbing aerosol on precipitation: Dynamic aspects in association with convective available potential energy and convective parameterization closure and dependence on aerosol heating profile, J. Geophys. Res., 109, D22103, doi:10.1029/2004JD004726.

Conant, W. C., J. H. Seinfeld, J. Wang, G. R. Carmichael, Y. Tang, I. Uno, P. J. Flatau, K. M. Markowicz, and P. K. Quinn (2003),A model for the radiative forcing during ACE-Asia derived from CIRPAS Twin Otter and R/V Ronald H. Brown data and comparison with observations, J. Geophys. Res., 108(D23), 8661,

doi:10.1029/2002JD003260.

Cowan, T., and W. Cai (2011), The impact of Asian and non-Asian anthropogenic aerosols on 20th century Asian summer monsoon, Geophys. Res. Lett., 38, L11703, doi:10.1029/2011GL047268.

Ding, Y., Y. Sun, Z. Wang, Y. Zhu, and Y. Song (2009), Inter-decadal variation of the summer precipitation in China and its association with decreasing Asian summer monsoon Part II: Possible causes, Int. J. Climatol., 29, 1926-1944, doi: 10.1002/joc.1759.

Ding, Y., Z. Wang, and Y. Sun (2008), Inter-decadal variation of the summer precipitation in East China and its association with decreasing Asian summer monsoon. Part I: Observed evidences, Int. J. Climatol., 28, 1139-1161, doi:10.1002/joc.1615.

Emmons, L. K., S. Walters, P. G. Hess, J.-F. Lamarque, G. G. Pfister, D. Fillmore, C. Granier, A. Guenther, D. Kinnison, T. Laepple, J. Orlando, X. Tie, G. Tyndall, C. Wiedinmyer, S. L. Baughcum, and S. Kloster (2010), Description and evaluation of the Model for Ozone and Related chemical Tracers, version 4 (MOZART-4), Geosci. Model Dev., 3, 43-67.

Ganguly, D., P. J. Rasch, H. Wang, and J. Yoon (2012), Fast and slow responses of the South Asian monsoon system to anthropogenic aerosols, Geophys. Res. Lett., 39, L18804, doi:10.1029/2012GL053043.

Gautam, R., N. C. Hsu, K. M. Lau, and M. Kafatos (2009), Aerosol and rainfall variability over the Indian monsoon region: distributions, trends and coupling, Ann. Geophys., 27, 3691-3703.

Gettelman, A., X. Liu, S. J. Ghan , H. Morrison, S. Park, A. J. Conley, S. A. Klein, J. Boyle, D. L. Mitchell , and J.-L. F. Li (2010), Global simulations of ice nucleation and ice supersaturation with an improved cloud scheme in the Community Atmosphere Model, J. Geophys. Res., 115, D18216, doi:10.1029/2009JD013797.

Gu, Y., K. N. Liou, Y. Xue, C. R. Mechoso, W. Li, and Y. Luo (2006), Climatic effects of different aerosol types in China simulated by the UCLA general circulation model, J. Geophys. Res., 111, D15201, doi:10.1029/2005JD006312.

Guo, L., E. J. Highwood, L. C. Shaffrey, and A. G. Turner (2013), The effect of regional changes in anthropogenic aerosols on rainfall of the East Asian Summer Monsoon, Atmos. Chem. Phys., 13, 1521-1534, doi:10.5194/acp-13-1521-2013.

Hansen J, M. Sato, and R. Ruedy (1997), Radiative forcing and climate response. J Geophys Res., 102, D6, 6831-6864.

He, B., Q. Bao, J. Li, G. Wu, Y. Liu, X. Wang, and Z. Sun (2013), Influences of external forcing changes on the summer cooling trend over East Asia, Clim. Change, 117, 829-841.

He, J., P. Zhao, C. Zhu, R. Zhang, X. Tang, L. Chen, and X. Zhou (2008), Discussion

of Some Problems as to the East Asian Subtropical Monsoon, Acta Meteor. Sinica, 22(4), 419-434.

Huang, Y., Chameides, W., and Dickinson, R.: Direct and indirect effects of anthropogenic aerosols on regional precipitation over east Asia, J. Geophys. Res., 112, D03212, doi:10.1029/2006JD007114, 2007.

Iacono, M. J., J. S. Delamere, E. J. Mlawer, M. W. Shephard, S. A. Clough, and W. D. Collins (2008), Radiative forcing by long-lived greenhouse gases: Calculations with the AER radiative transfer models, J. Geophys. Res., 113, D13103, doi:10.1029/2008JD009944.

IPCC, 2007: Climate Change 2007: Synthesis Report. Contribution of Working Groups I, II and III to the Fourth Assessment Report of the Intergovernmental Panel on Climate Change [Core Writing Team, Pachauri, R.K and Reisinger, A. (eds.)]. IPCC, Geneva, Switzerland, 104 pp.

Ji, Z., S. Kang, D. Zhang, C. Zhu, J. Wu, and Y. Xu (2011), Simulation of the anthropogenic aerosols over South Asia and their effects on Indian summer monsoon, Clim. Dyn., 36, 1633-1647, doi: 10.1007/s00382-010-0982-0.

Jiang, D., and H. Wang (2005), Natural interdecadal weakening of East Asian summer monsoon in the late 20th century, Chinese Science Bulletin, 50, 1923-1929, doi:10.1360/982005-36.

Jiang, Y., X. Liu, X.-Q. Yang, and M. Wang (2013), A numerical study of the effect of

different aerosol types on East Asian summer clouds and precipitation, Atmos. Environ., 70, 51-63, doi:10.1016/j.atmosenv.2012.12.039.

Jiang, Y., X.-Q. Yang, and X. Liu (2015), Seasonality in anthropogenic aerosol effects on East Asian climate simulated with CAM5, J. Geophys. Res. Atmos., 120, doi:10.1002/2015JD023451.

Jin, Q., X.-Q. Yang, X. Sun, and J. Fang (2013), East Asian summer monsoon circulation structure controlled by feedback of condensational heating. Clim. Dyn., 41, 1885-1897, doi:10.1007/s00382-012-1620-9.

Junker, C., and C. Liousse (2008), A global emission inventory of carbonaceous aerosol from historic records of fossil fuel and biofuel consumption for the period 1860-1997, Atmos. Chem. Phys., 8, 1195-1207.

Kalnay, E., M. Kanamitsu, R. Kistler, W. Collins, D. Deaven, L. Gandin, M. Iredell, S. Saha, G. White, J. Woollen, Y. Zhu, A. Leetmaa, and B. Reynolds (1996), The NCEP/NCAR 40-year reanalysis project, Bull. Am. Meterol. Soc., 77, 437-471.

Kim, M.-K., W. K. M. Lau, K.-M. Kim, and W.-S. Lee (2007), A GCM study of effects of radiative forcing of sulfate aerosol on large scale circulation and rainfall in East Asia during boreal spring, Geophys. Res. Lett., 34, L24701, doi:10.1029/2007GL031683.

Lack, D. A., X. X. Tie, N. D. Bofinger, A. N. Wiegand, and S. Madronich (2004), Seasonal variability of secondary organic aerosol: A global modeling study, J.

Geophys. Res., 109, D03203, doi:10.1029/2003JD003418.

Lamarque, J. F., T. Bond, V. Eyring, C. Granier, A. Heil, Z. Klimont, D. Lee, C. Liousse, A. Mieville, B. Owen, M. G. Schultz, D. Shindell, S. J. Smith, E. Stehfest, J. Van Aardenne, O. R. Cooper, M. Kainuma, N. Mahowald, J. R. McConnell, V. Naik, K. Riahi, and D. P. van Vuuren. (2010), Historical (1850-2000) gridded anthropogenic and biomass burning emissions of reactive gases and aerosols: methodology and application, Atmos. Chem. Phys., 10(15), 7017-7039, doi:10.5194/acp-10-7017-2010.

Lau, K. M., M. K. Kim, and K. M. Kim (2006), Asian summer monsoon anomalies induced by aerosol direct forcing: the role of the Tibetan Plateau, Clim. Dyn., 26, 855-864, doi: 10.1007/s00382-006-0114-z

Lau, K.-M. and K.-M. Kim (2006), Observational relationships between aerosol and Asian monsoon rainfall, and circulation, Geophys. Res. Lett., 33, L21810, doi:10.1029/2006GL027546.

Lau, W. K. M., and K.-M. Kim (2010), Fingerprinting the impacts of aerosols on long-term trends of the Indian summer monsoon regional rainfall, Geophys. Res. Lett., 37, L16705, doi:10.1029/2010GL043255.

Lefohn, A. S., J. D. Husar, and R. B. Husar (1999), Estimating historical anthropogenic global sulfur emission patterns for the period 1850-1990, Atmos. Environ., 33, 3435-3444.

Lei, Y., B. Hoskins, and J. Slingo (2011), Exploring the interplay between natural decadal variability and anthropogenic climate change in summer rainfall over China. Part I: observational evidence, J. Clim., 24, 4584-4599, doi: 10.1175/2010JCLI3794.1.

Lei, Y., B. Hoskins, and J. Slingo (2011), Natural variability of summer rainfall over China in HadCM3, Clim. Dyn., 42, 417-432.

Li, H., A. Dai, T. Zhou, and J. Lu (2010a), Responses of East Asian summer monsoon to historical SST and atmospheric forcing during 1950-2000, Clim. Dyn., 34, 501-514, doi: 10.1007/s00382-008-0482-7.

Li, J., Z. Wu, Z. Jiang and J. He (2010b), Can global warming strengthen the East Asian summer monsoon? J. Clim., 23, 6696-6705, doi: 10.1175/2010JCLI3434.1.

Liao, H., P. J. Adams, S. H. Chung, J. H. Seinfeld, L. J. Mickley, and D. J. Jacob (2003), Interactions between tropospheric chemistry and aerosols in a unified general circulation model, J. Geophys. Res., 108, D1, 4001, doi:10.1029/2001JD001260

Liao, H., W. Chang, and Y. Yang (2015), Climatic effects of air pollutants over china: A review, Adv. Atmos. Sci., 32(1), 115-139, doi:10.1007/s00376-014-0013-x.

Liu, Y., G. Wu, and R. Ren (2004), Relationship between the Subtropical Anticyclone and Diabatic Heating. J. Clim., 17, 682-698.

Liu, Y., G. Wu, J. Hong, B. Dong, A. Duan, Q. Bao, and L. Zhou (2012), Revisiting Asian monsoon formation and change associated with Tibetan Plateau forcing: II. Change, Clim. Dyn., 39, 1183-1195, doi: 10.1007/s00382-012-1335-y.

Liu, Y., J. Sun, and B. Yang (2009), The effects of black carbon and sulphate aerosols in China regions on East Asia monsoons, Tellus, 61B, 642-656, doi:10.1111/j.1600-0889.2009.00427.x.

Mahmood, R., and S. Li (2013a), Remote influence of South Asian black carbon aerosols on East Asian climate, Int. J. Climatol., doi:10.1002/joc.3664.

Mahmood, R., and S. Li (2013b), Delay in the onset of South Asian summer monsoon induced by local black carbon in an AGCM, Theor. Appl. Climatol., 111, 529-536, doi:10.1007/s00704-012-0681-3.

Mahmood, R., and S. Li, (2011), Modeled influence of East Asian black carbon on inter-decadal shifts in East China summer rainfall, Atmos. Oceanic Sci. Lett., 4, 349-355.

Mahowald, N., J.-F. Lamarque, X. X. Tie, and E. Wolff (2006a), Seasalt aerosol response to climate change: Last glacial maximum, preindustrial, and doubled carbon dioxide climates, J. Geophys. Res., 111, D05303, doi:10.1029/2005JD006459

Mahowald, N. M., D. R. Muhs, S. Levis, P. J. Rasch, M. Yoshioka, C. S. Zender, and C. Luo (2006b), Change in atmospheric mineral aerosols in response to climate:

Last glacial period, pre-industrial, modern, and doubled carbon dioxide climates, J. Geophys. Res., Atmospheres, 111, D10202, doi:10.1029/2005JD006653

Martin, A. C., T. N. Krishnamurti, and W. K. M. Lau (2013), Absorbing aerosol-induced change in the early monsoon Arabian Sea low-level jet: Modeled transfer from anomalous heating to nondivergent kinetic energy, J. Geophys. Res. Atmos., 118, 12566-12576, doi:10.1002/2013JD019808.

Meehl, G., J. Arblaster, and W. Collins, (2008), Effects of black carbon aerosols on the Indian monsoon, J. Clim., 21, 2869-2882.

Menon, S., J. Hansen, L. Nazarenko, and Y. Luo (2002), Climate effects of black carbon aerosols in China and India, Science, 297, 2250-2253.

Ming, Y., V. Ramaswamy, and G. Persad (2010), Two opposing effects of absorbing aerosols on global-mean precipitation, Geophys. Res. Lett., 37, L13701, doi:10.1029/2010GL042895.

Morrison, H., and A. Gettelman (2008), A new two-moment bulk stratiform cloud microphysics scheme in the Community Atmosphere Model, version 3 (CAM3). Part I: Description and numerical tests, J. Clim., 21, 3642-3659, doi: 10.1175/2008JCLI2105.1.

Neale, R. B., et al. (2010), Description of the NCAR Community Atmosphere Model (CAM5.0), NCAR/TN-486+STR, NCAR, Boulder, Colo. [Available at http://www.cesm.ucar.edu/models/cesm1.0/cam/docs/description/cam5_desc.pdf.

]

Qi, L., J. He, Z. Zhang, and J. Song (2008), Seasonal cycle of the zonal land-sea thermal contrast and East Asian subtropical monsoon circulation, Chinese Science Bulletin, 53(1): 131-136.

Ramanathan, V., C. Chung, D. Kim, T. Bettge, L. Buja, J. T. Kiehl, W. M. Washington, Q. Fu, D. R. Sikka, and M. Wild (2005), Atmospheric brown clouds: Impacts on South Asian climate and hydrological cycle, Proc. Natl. Acad. Sci. U. S. A., 102, 5326-5333, doi:10.1073/pnas.0500656102.

Ramanathan, V., P. J. Crutzen, J. T. Kiehl, and D. Rosenfeld (2001), Aerosols, climate, and the hydrological cycle, Science, 294, 2119-2124, doi: 10.1126/science.1064034.

Randles, C. A., and V. Ramaswamy (2008), Absorbing aerosols over Asia: A Geophysical Fluid Dynamics Laboratory general circulation model sensitivity study of model response to aerosol optical depth and aerosol absorption, J. Geophys. Res., 113, D21203, doi:10.1029/2008JD010140.

Schulz, M., Textor, C., Kinne, S., Balkanski, Y., Bauer, S., Berntse, T., Berglen, T., Boucher, O., Dentener, F., Guibert, S., Isaksen, I.S.A., Iversen, T., Koch, D., Kirkevag, A., Liu, X., Montanaro, V., Myhre, G., Penner, J., Pitari, G., Reddy, S., Seland, O., Stier, P., Takemura, T., (2006), Radiative forcing by aerosols as derived from the AeroCom present-day and pre-industrial simulations, Atmos.

Chem. Phys., 6, 5225-5246.

Smith, S. J., J. van Aardenne, Z. Klimont, R. J. Andres, A. Volke, and S. Delgado Arias (2011), Anthropogenic sulfur dioxide emissions: 1850-2005, Atmos. Chem. Phys., 11, 1101-1116, doi:10.5194/acp-11-1101-2011.

Song, F., T. Zhou, and Y. Qian (2014), Responses of East Asian summer monsoon to natural and anthropogenic forcings in the 17 latest CMIP5 models, Geophys. Res. Lett., 41, doi:10.1002/2013GL058705.

Song, F. and T. Zhou, (2014), Interannual Variability of East Asian Summer Monsoon Simulated by CMIP3 and CMIP5 AGCMs: Skill Dependence on Indian Ocean-Western Pacific Anticyclone Teleconnection, J. Climate, 27, 1679-1697.

Streets, D. G., C. Yu, Y. Wu, M. Chin, Z. Zhao, T. Hayasaka, and G. Shi (2008), Aerosol trends over China, 1980-2000, Atmos. Res., 88, 174-182, doi:10.1016/j.atmosres.2007.10.016.

Tao, S., and L. Chen (1987), A review on the East Asian Summer monsoon // Krishnamurti, C University Press, 60-92

Tie, X., G. Brasseur, L. Emmons, L. Horowitz, and D. Kinnison (2001), Effects of aerosols on tropospheric oxidants: A global model study. J. Geophys. Res., 106. D19: 22931-22964.

Tie, X., S. Madronich, S. Walters, D. P. Edwards, P. Ginoux, N. Mahowald, R. Zhang,

C. Lou, and G. Brasseur (2005), Assessment of the global impact of aerosols on tropospheric oxidants, J. Geophys. Res., 110, D03204, doi:10.1029/2004JD005359

Ueda, H., A. Iwai, K. Kuwako, and M. E. Hori (2006), Impact of anthropogenic forcing on the Asian summer monsoon as simulated by eight GCMs, Geophys. Res. Lett., 33, L06703, doi:10.1029/2005GL025336.

Wang, C. (2007), Impact of direct radiative forcing of black carbon aerosols on tropical convective precipitation, Geophys. Res. Lett., 34, L05709, doi:10.1029/2006GL028416.

Wang, C., D. Kim, A. M. L. Ekman, M. C. Barth, and P. J. Rasch (2009), Impact of anthropogenic aerosols on Indian summer monsoon, Geophys. Res. Lett., 36, L21704, doi:10.1029/2009GL040114.

Wang, D., B. Zhu, Z. Jiang, X. Yang, and T. Zhu (2014), Direct effect of sulfate aerosols on the progress of the East Asian subtropical monsoon, Chinese Journal of Atmospheric Sciences (in Chinese), 38(5), 897-908, doi:10.3878/j.issn.1006-9895.1403.13193.

Wang, H. (2001), The weakening of the Asian monsoon circulation after the end of 1970's, Adv. Atmos. Sci., 18, 376-386.

Wang, H. (2002), Instability of the East Asian summer monsoon-ENSO relations, Adv. Atmos. Sci.,19, 1-11.

Wang, T., H. Wang, H. Ottera, Y. Gao, L. Suo, T. Furevik, and L. Yu (2013), Anthropogenic agent implicated as a prime driver of shift in precipitation in eastern China in the late 1970s, Atmos. Chem. Phys., 13, 12433-12450, doi:10.5194/acp-13-12433-2013.

Wu, G., Y. Liu, B. Dong, X. Liang, A. Duan, Q. Bao, and J. Yu (2012), Revisiting Asian monsoon formation and change associated with Tibetan Plateau forcing: I. Formation, Clim. Dyn., 39, 1169-1181, doi: 10.1007/s00382-012-1334-z.

Xu, M., C.-P. Chang, C. Fu, Y. Qi, A. Robock, D. Robinson, and H. Zhang (2006), Steady decline of east Asian monsoon winds, 1969-2000: Evidence from direct ground measurements of wind speed, J. Geophys. Res., 111, D24111, doi:10.1029/2006JD007337.

Xu, Q. (2001), Abrupt change of the mid-summer climate in central east China by the influence of atmospheric pollution, Atmos. Environ., 35, 5029-5040.

Xue, F. (2001), Interannual to interdecadal variation of East Asian summer monsoon and its association with the global atmospheric circulation and sea surface temperature, Adv. Atmos. Sci., 18, 567-575.

Yang, F., and K. Lau (2004), Trend and variability of China precipitation in spring and summer: Linkage to sea surface temperatures, Int. J. Climatol., 24, 1625-1644.

Yeh, T., S. Dao, and M. Li (1959), The Abrupt Change of Circulation over the Northern Hemisphere During June and October // The Atmospher

Motion. New York: The Rockefelher Institute Press in Association with Oxford University Press, 246-267

Yu, R., B. Wang, and T. Zhou (2004), Tropospheric cooling and summer monsoon weakening trend over East Asia, Geophys. Res. Lett., 31, L22212, doi:10.1029/2004GL021270.

Zhang, H., Z. Wang, Z. Wang, Q. Liu, S. Gong, X. Zhang, Z. Shen, P. Lu, X. Wei, H. Che, and L. Li (2012), Simulation of direct radiative forcing of aerosols and their effects on East Asian climate using an interactive AGCM-aerosol coupled system, Clim. Dyn., 38, 1675-1693, doi:10.1007/s00382-011-1131-0.

Zhao, P., R. Zhang, J. Liu, X. Zhou, and J. He (2007), Onset of southwesterly wind over eastern China and associated atmospheric circulation and rainfall, Clim. Dyn., 28, 797-811, doi: 10.1007/s00382-006-0212-y.

Zhao, P., X. Zhou, L. Chen, and J. He (2009), Characteristics of subtropical monsoon and rainfall over eastern China and western north Pacific, Acta Meteor. Sinica, 23(6), 649-655.

Zhou, T., and L, Zou (2010), Understanding the Predictability of East Asian Summer Monsoon from the Reproduction of Land--Sea Thermal Contrast Change in AMIP-Type Simulation, J. Clim., 23, 6009-6026, doi: 10.1175/2010JCLI3546.1.

Zhou, T., D. Gong, J. Li, and B, Li (2009), Detecting and understanding the multi-decadal variability of the East Asian Summer Monsoon-recent progress

and state of affairs, Meteorol. Z., 18, 455-467, doi: 10.1127/0941-2948/2009/0396.

Zhou, Y., A. Huang, J. Jiang, and M. La (2014), Modeled interaction between the subseasonal evolving of the East Asian summer monsoon and the direct effect of anthropogenic sulfate, J. Geophys. Res. Atmos., 119, 1993-2016, doi:10.1002/2013JD020612.

Zhu, C., B. Wang, W. Qian, and B. Zhang (2012), Recent weakening of northern East Asian summer monsoon: A possible response to global warming, Geophys. Res. Lett., 39, L09701, doi:10.1029/2012GL051155.

Zhu, C., X. Zhou, P. Zhao, L. Chen, and J. He (2011), Onset of East Asian Sub-tropical Summer Monsoon and Rainy Season in China, Sci. China Earth Sci., 54, 12, 1845-1853, doi:10.1007/s11430-011-4284-0.

Zhu, Q., J. He, and P. Wang (1986), A study of circulation differences between East-Asian and Indian summer monsoons with their interaction, Adv. Atmos. Sci., 3(4), 466-477.

Table 1. Definition of the simulations conducted in the study

Simulation	Specification
Ctrl	CAM5.1 contains all types of aerosol direct and indirect radiative processes with climatological SST
nSO4de	Ctrl run without the DE of sulfate
nBCde	Ctrl run without the DE of BC
nSO4BCde	Ctrl run without the DE of sulfate and BC

Table 2.The time of transitions and changes of 850hPa and 500hPa zonal land-sea thermal contrast (ZTC) and 850hPa meridional wind (V)*

Experiment	Transition time (pentad)											
	850hPa ZTC				500hPa ZTC				850hPa V			
	1st	Δp	2nd	Δp	1st	Δp	2nd	Δp	1st	Δp	2nd	Δp
Ctrl	16th	-	55th	-	15th	-	55th	-	18th	-	56th	-
nSO4de	15th	1 p	56th	-1 p	15th	-	55th	-	17th	1 p	57th	-1 p
nBCde	15th	1 p	55th	-	16th	-1 p	55th	-	19th	-1 p	57th	-1 p
nSO4BCde	14th	2 p	56th	-1 p	16th	-1 p	55th	-	19th	-1 p	58th	-2 p

*Δp is the change of pentads compared with the Ctrl experiment in the simulation experiments. Early is positive, p is pentad.

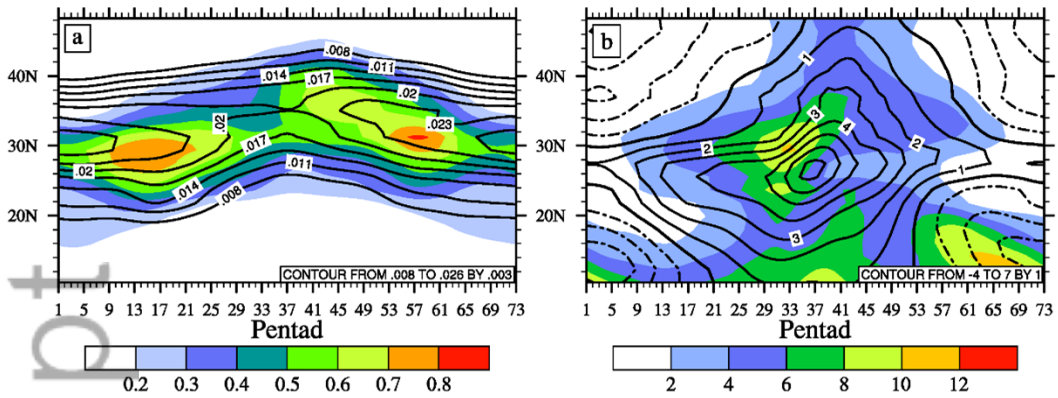

Fig. 1. Time-latitude cross section of (a) sulfate (shade) and BC (contour) aerosol optical depth (AOD) and (b) the total precipitation rate (shade, $mm \cdot d^{-1}$) and meridional wind (contour, $m \cdot s^{-1}$) at 850 hPa along the longitudes 105°-120°E from the Ctrl experiment.

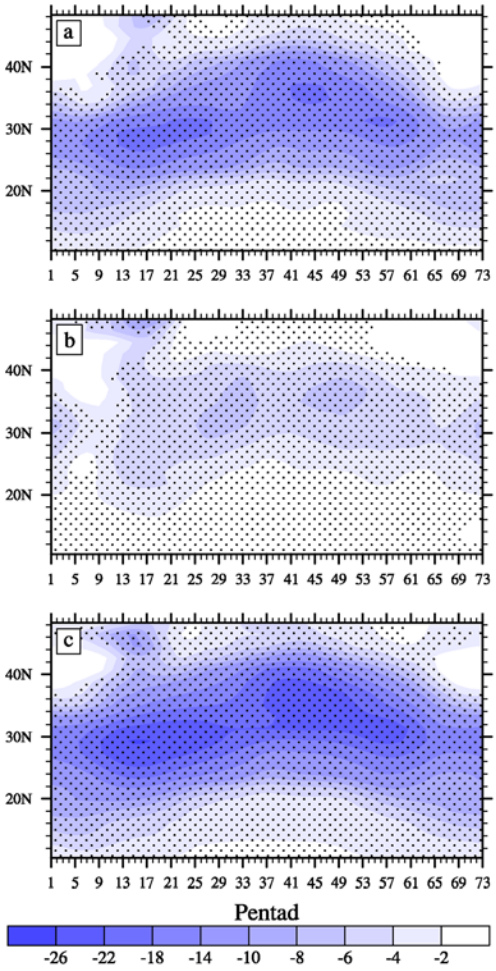

Fig. 2. Time-latitude cross section of clear-sky net solar radiation flux at surface (unit: $W \cdot m^{-2}$) changes due to the direct effects of sulfate (a), BC (b) and the combination of sulfate and BC aerosol (c) along the longitudes 105°-120°E. The dotted areas indicate statistical significance above the 90% level.

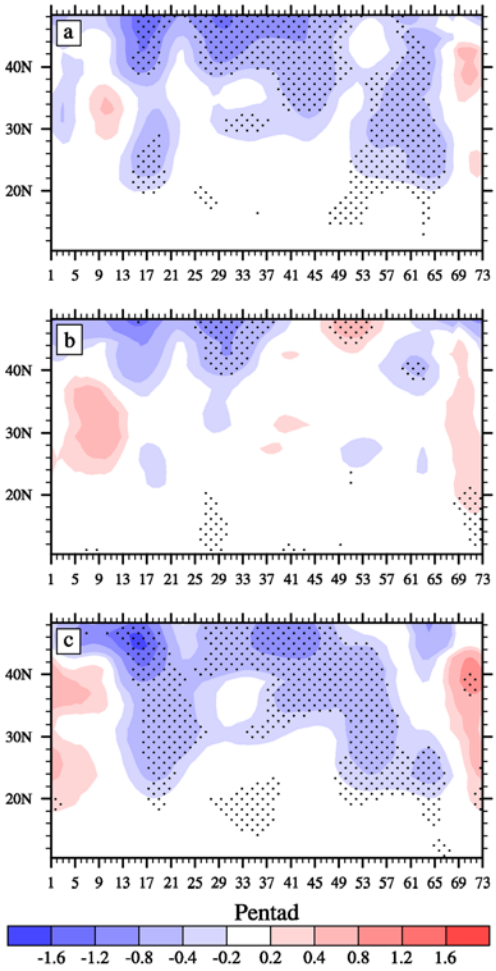

Fig. 3. Time-latitude cross section of surface air temperature (unit: K) changes due to the direct effects of sulfate (a), BC (b) and the combination of sulfate and BC aerosol (c) along the longitudes 105°-120°E. The dotted areas indicate statistical significance above the 90% level.

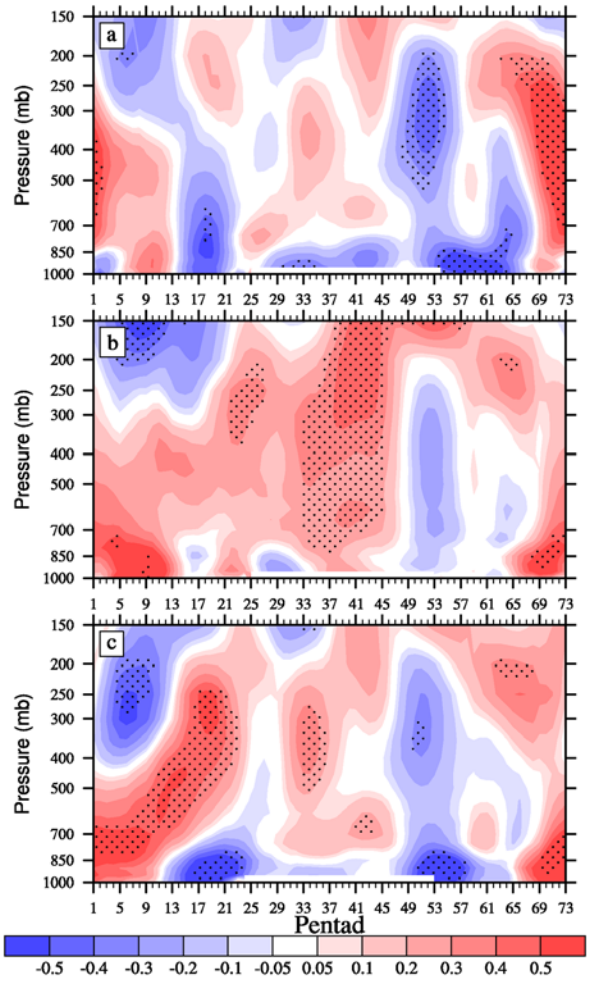

Fig. 4. Time-altitude cross section of temperature (unit: K) changes due to the aerosol direct effects of sulfate (a), BC (b) and the combination of sulfate and BC aerosol (c) over the subtropical continent (27.5°-32.5°N, 105°-120°E). The dotted areas indicate statistical significance above the 90% level.

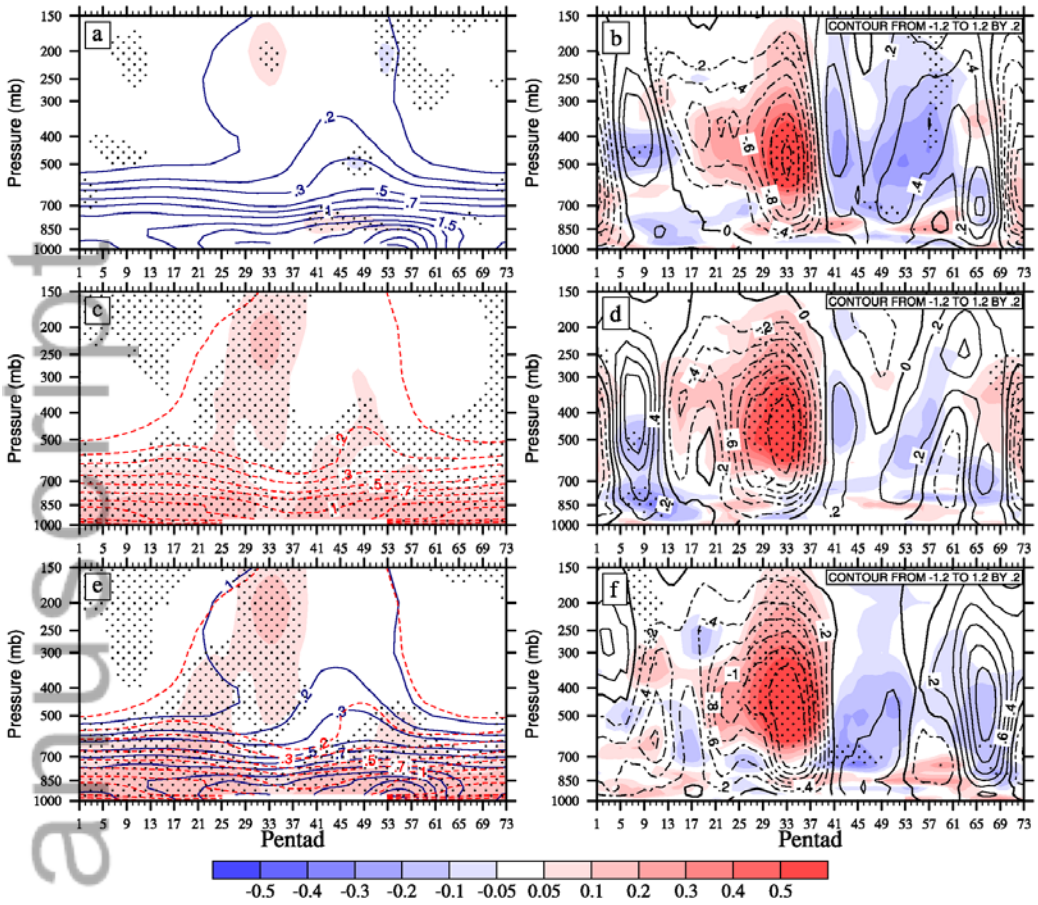

Fig. 5. Time-altitude cross section of (left) shortwave heating rate (QRS) (shade, unit: K·d^{-1}) changes due to aerosol direct effects and the aerosol concentration (contour, unit: μg·m-3) and (right) condensational heating rate from moisture processes (DTCOND, unit: K·d^{-1}) and vertical velocity (contour, unit: 100 Pa·s^{-1}) changes due to aerosol direct effects over the subtropical continent (27.5°-32.5°N, 105°-120°E) of sulfate (a, b), BC (c, d) and combination of sulfate and BC aerosol (e, f). The navy blue line shows the concentration of sulfate, and the red line shows the concentration of BC. The dotted areas indicate statistical significance of the change of the QRS (left)

and DTCOND (right) above the 90% level.

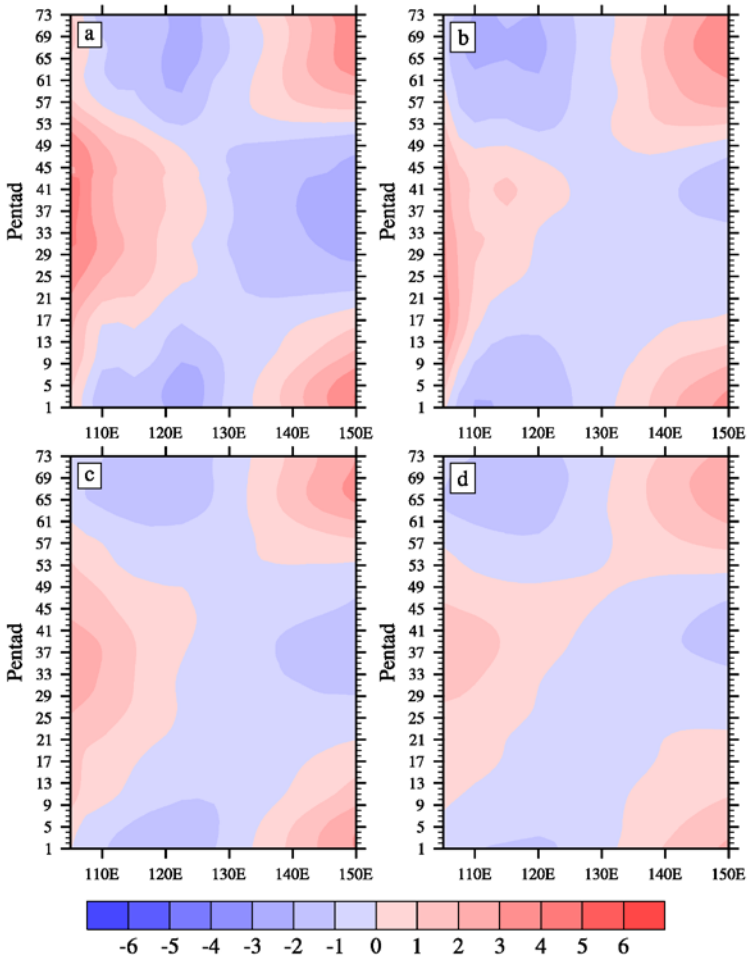

Fig. 6. Evolution of air temperature latitudinal deviation (TLD, unit: K) at 850 hPa (a, b) and 500 hPa (c, d) in the subtropics (27.5°-32.5°N) from (left) Ctrl experiment and (right) NCEP/NCAR reanalysis. TLD is defined as the discrepancy between the temperature at a given longitude and the mean temperature averaged over 105°-150°E at some selected latitudes.

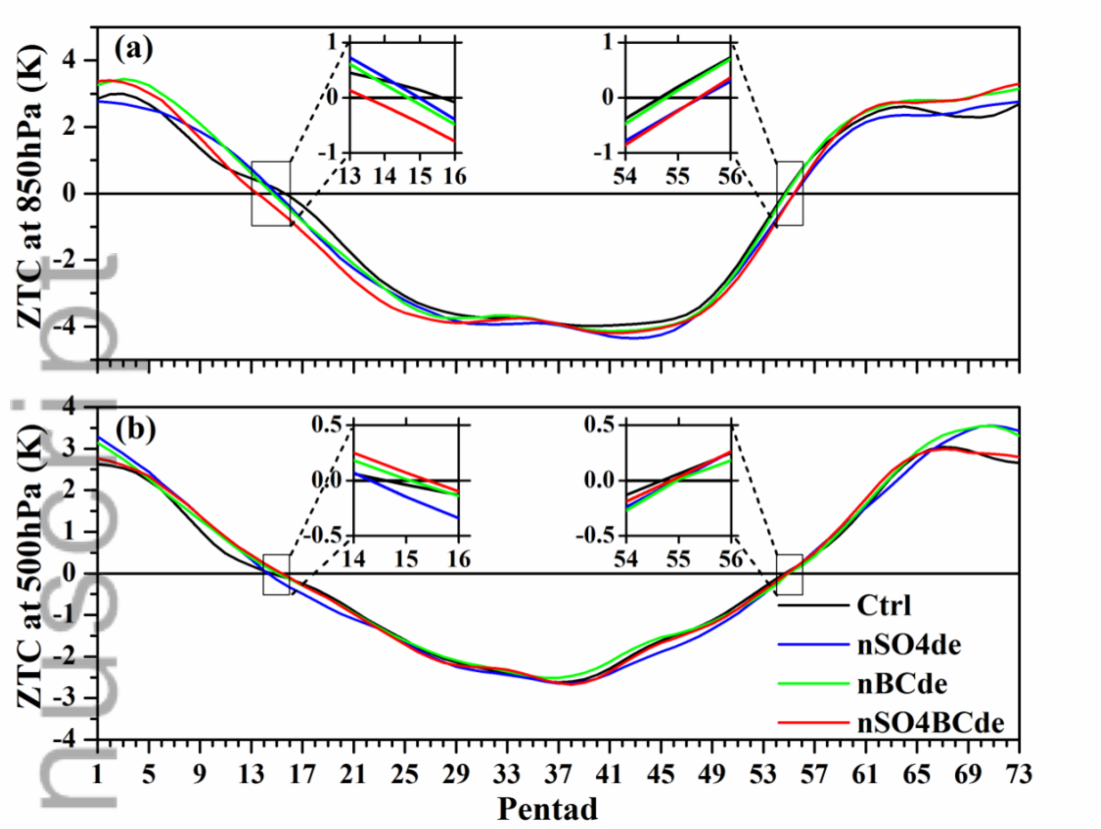

Fig. 7. The temporal evolution of zonal land-sea temperature contrast (ZTC, unit: K) at 850hPa (a) and 500hPa (b) at a latitude of 30°N in the simulation experiments. ZTC is defined as the temperature difference between the western Pacific Ocean (130°-150°E) and the East Asia continent (105°-120°E).

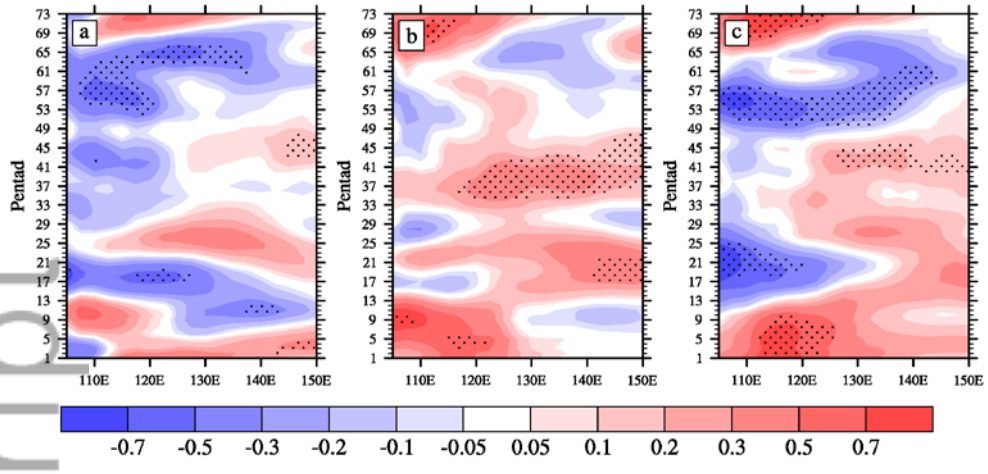

Fig. 8. Time-longitude cross section of air temperature (unit: K) changes at 850hPa due to the direct effects of sulfate (a), BC (b) and the combination of sulfate and BC aerosol (c) along the 30°N latitude. The dotted areas indicate statistical significance above the 90% level.

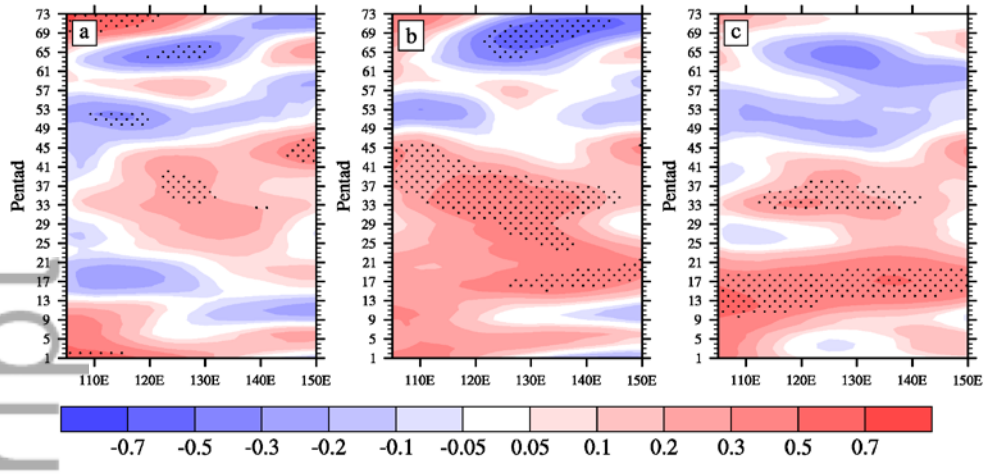

Fig. 9. Same as Fig. 8, but for 500hPa.

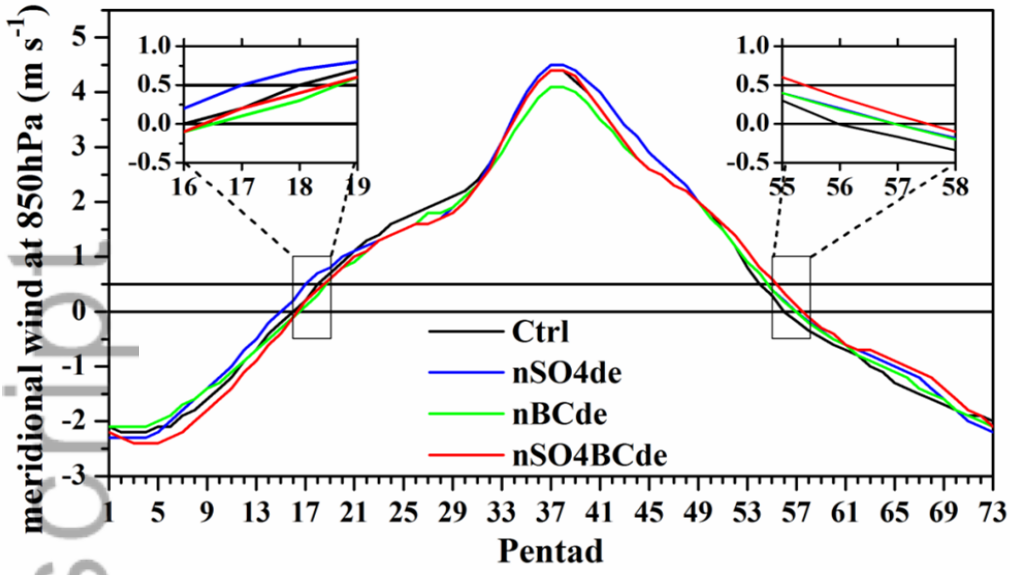

Fig. 10. The temporal evolution of meridional wind (unit: $m \cdot s^{-1}$) at 850hPa over the subtropics (27.5°-32.5°N, 110°-140°E) of simulation experiments.

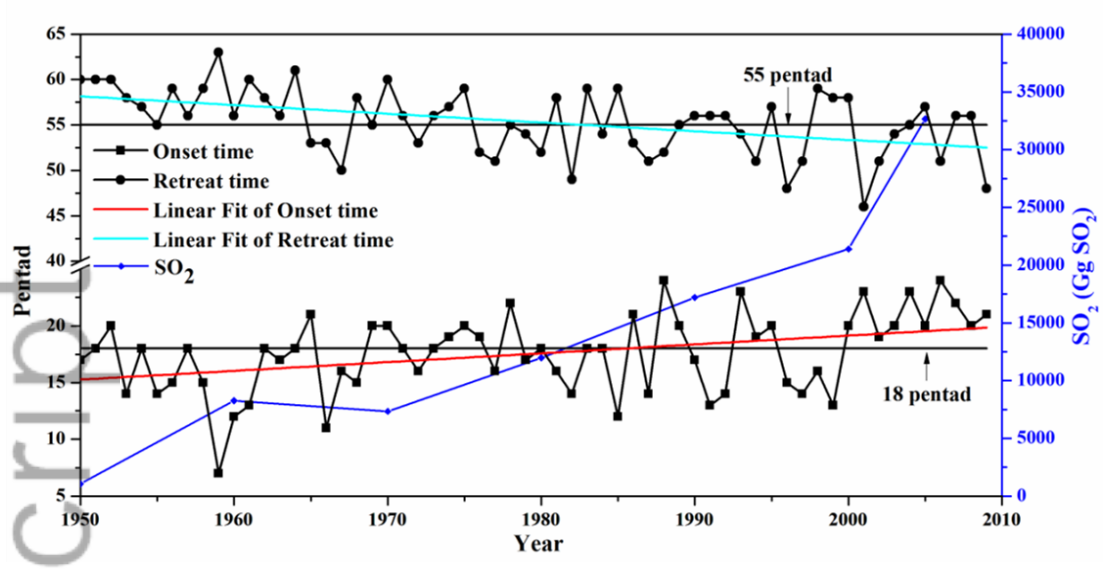

Fig. 11. Onset (black line with circles) and retreat time (black line with squares) of EASSM from 1950-2009 of the NCEP/NCAR reanalysis and the total SO_2 emissions estimated for a decade over China (blue line with diamonds, Unit: $Gg{\cdot}SO_2$; emission data is from *Smith et al.* [2011]). The average onset and retreat time are around 18th and 55th pentad (black line) and the red and cyan lines show the linear trend of onset and retreat times.

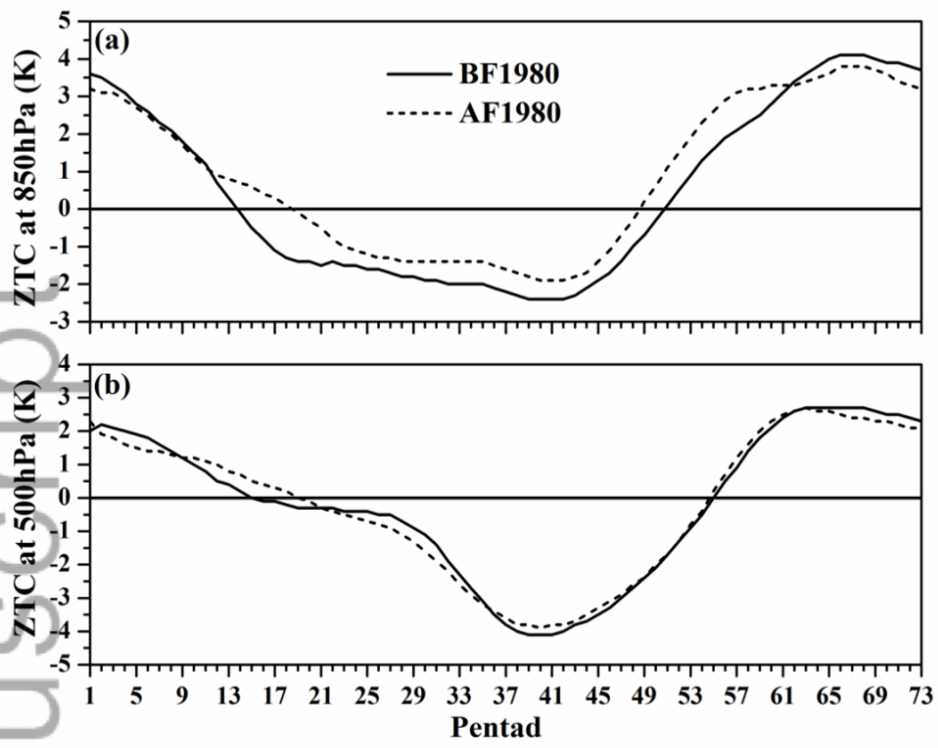

Fig. 12. The temporal evolution of zonal land-sea temperature contrast (ZTC, unit: K) at 850hPa (a) and 500hPa (b) at a latitude of 30N in the NCEP/NCAR reanalysis.

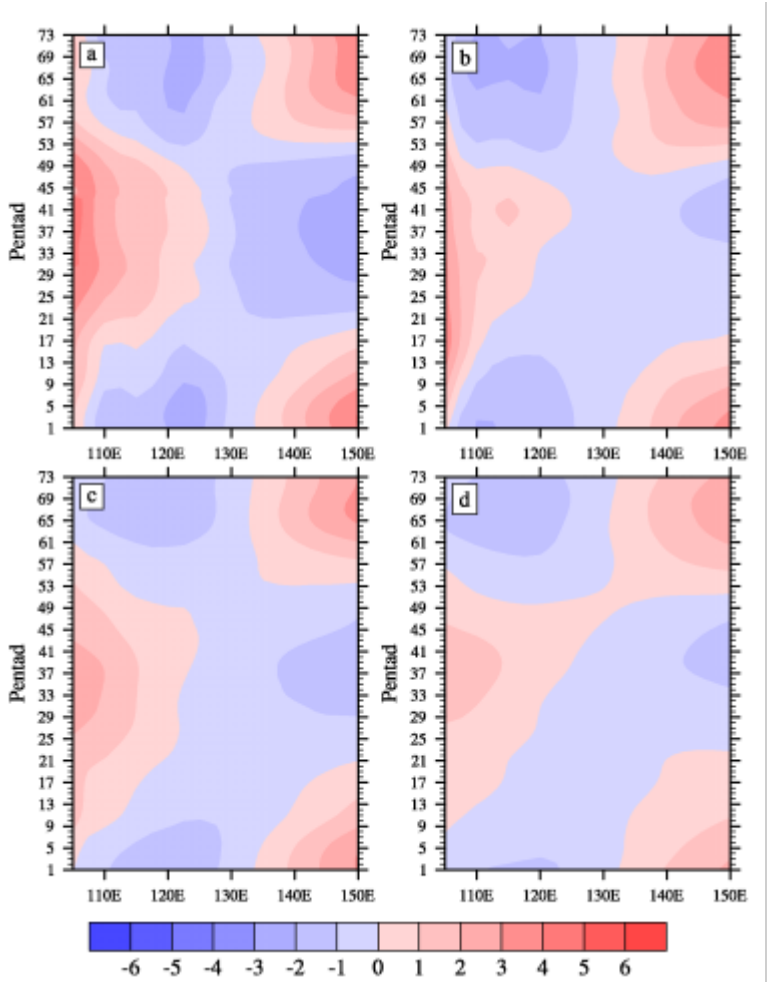

2015JD024574-f00-z-.tif

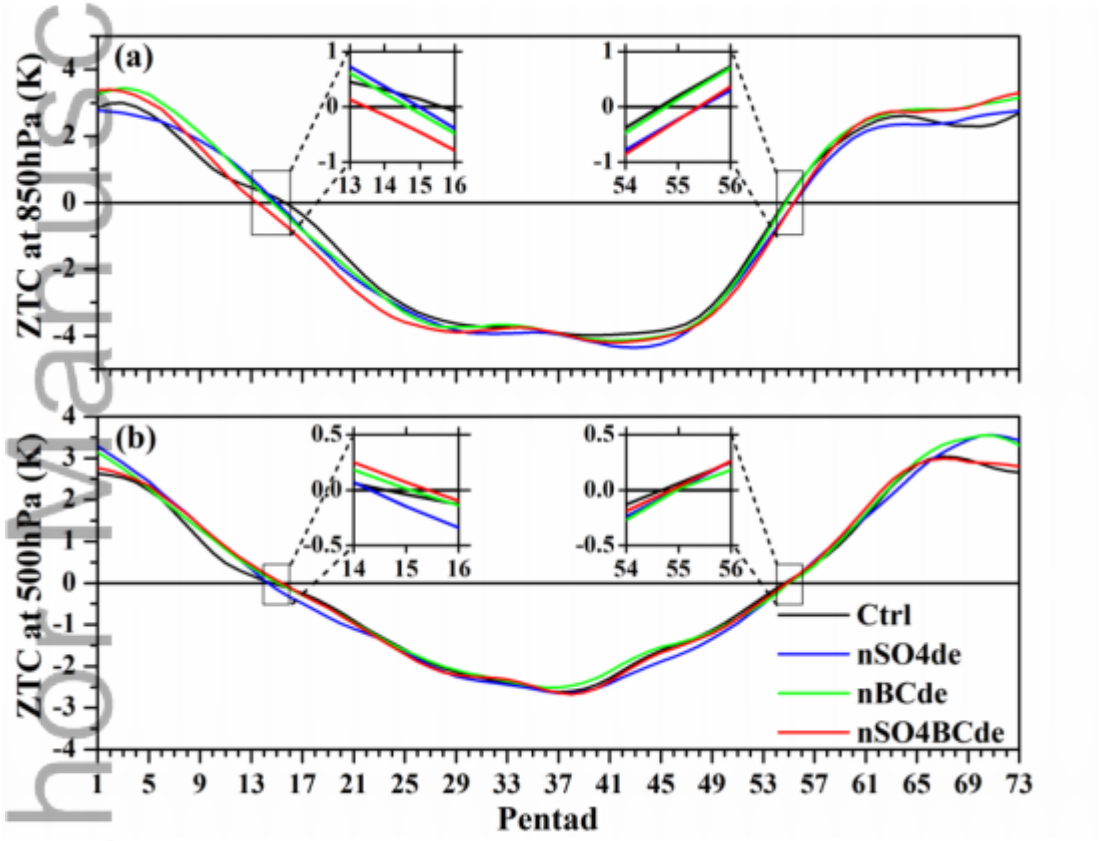

2015JD024574-f01-z-.tif

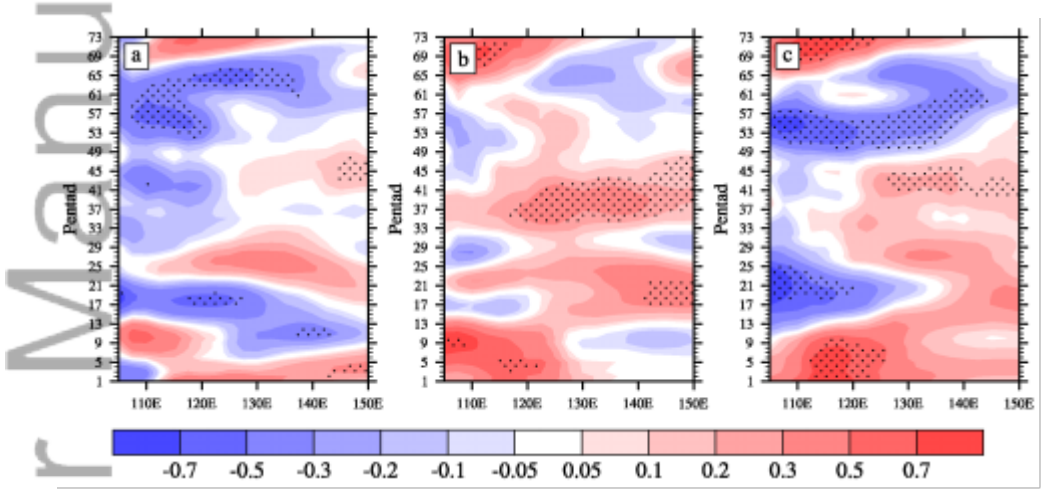

2015JD024574-f02-z-.tif

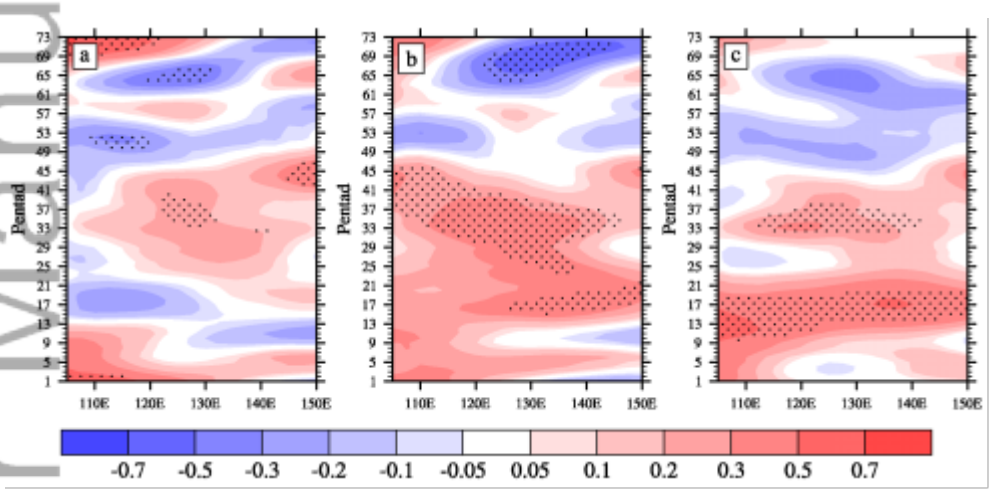

2015JD024574-f03-z-.tif

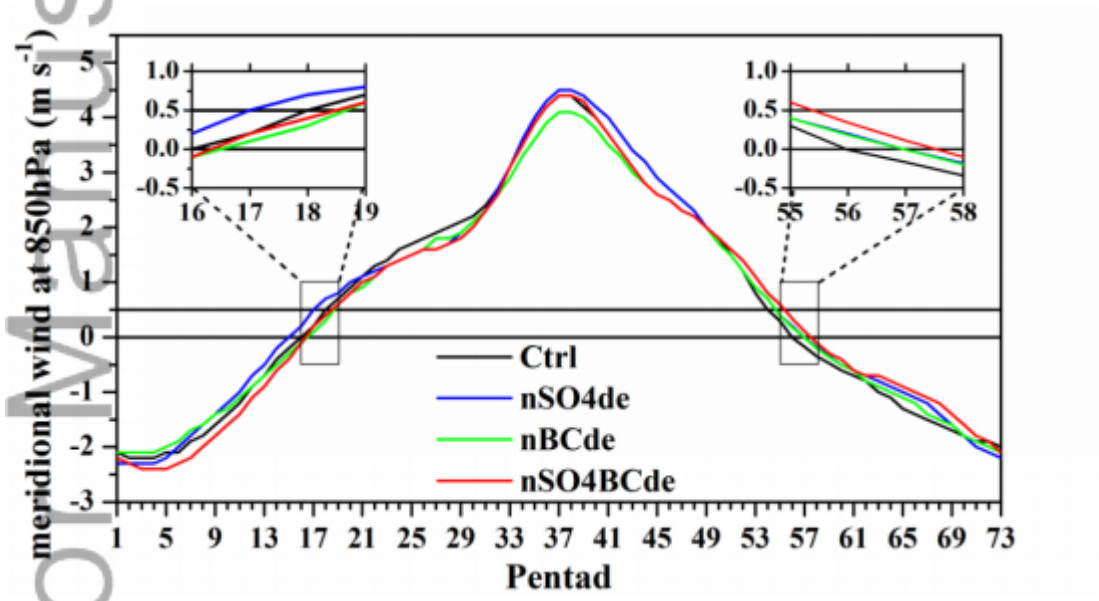

2015JD024574-f04-z-.tif

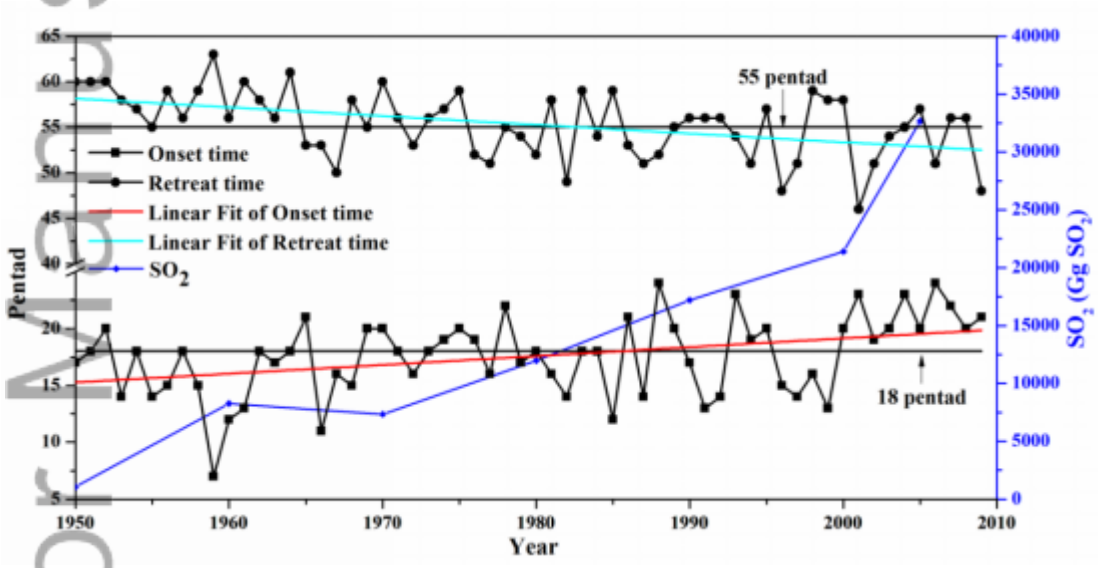

2015JD024574-f05-z-.tif

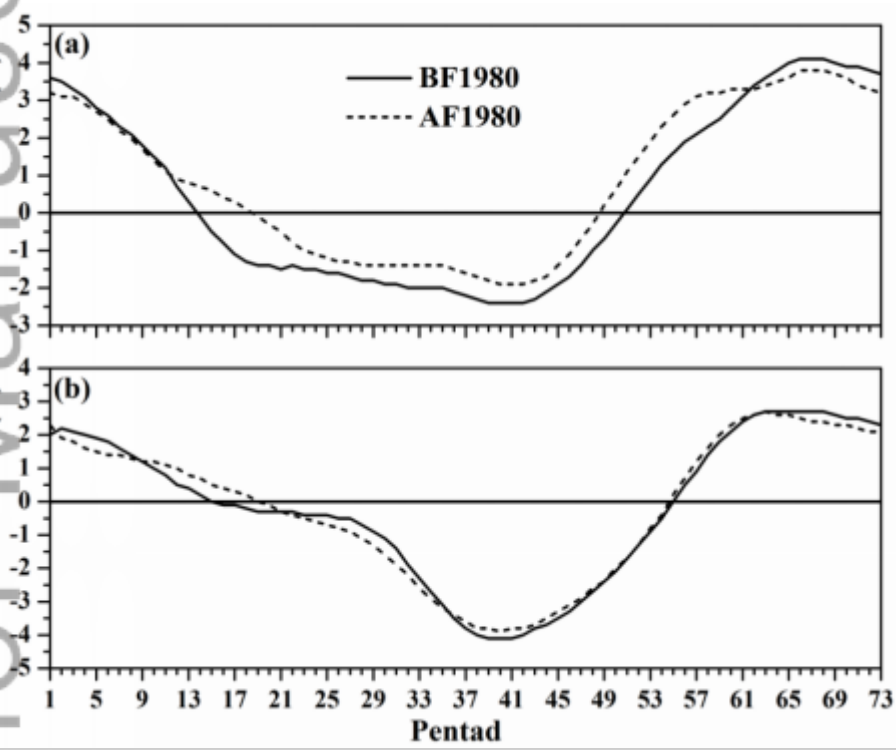

2015JD024574-f06-z-.tif

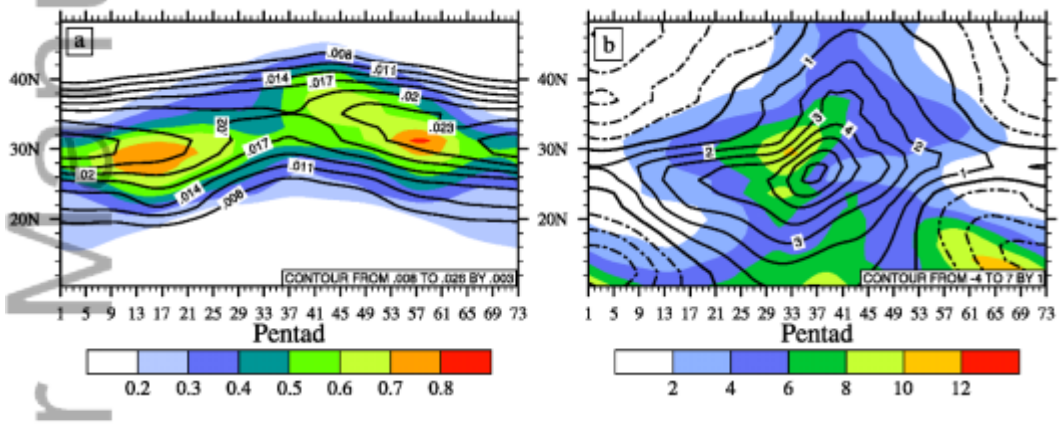

2015JD024574-f07-z-.tif

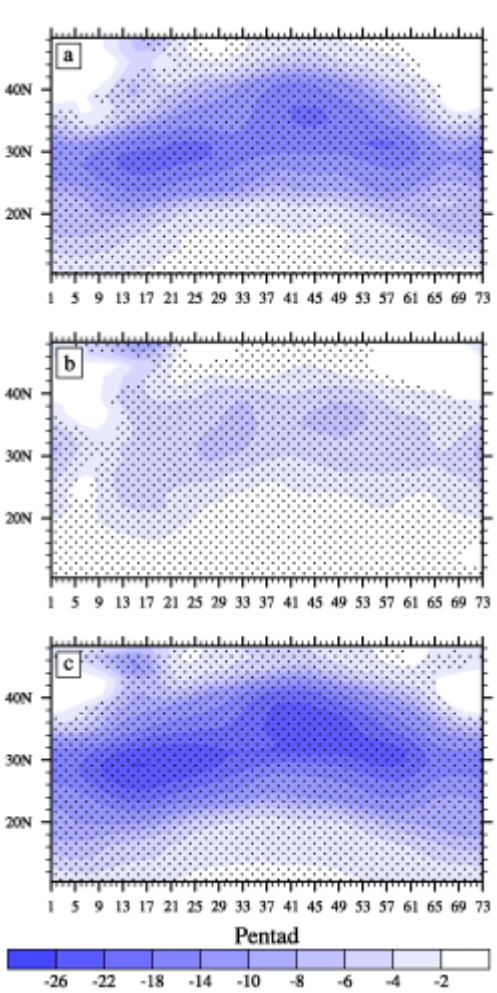

2015JD024574-f08-z-.tif

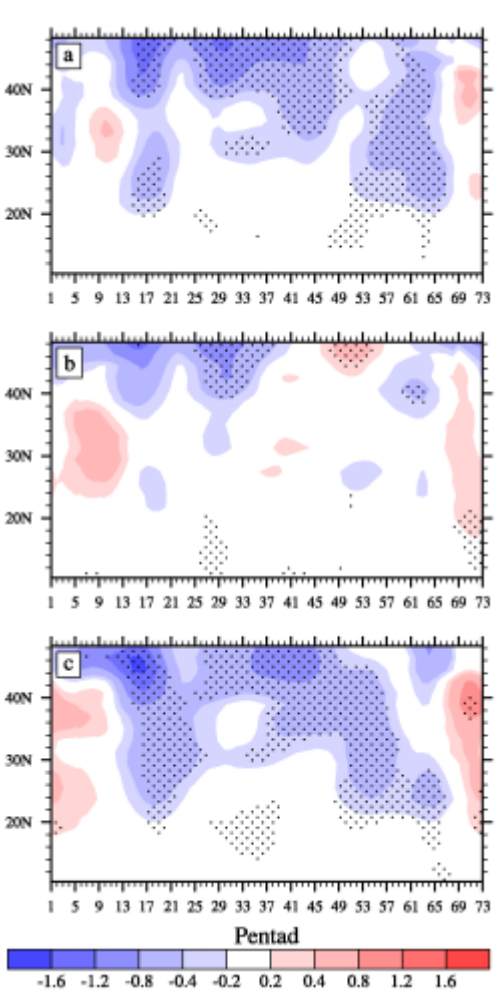

2015JD024574-f09-z-.tif

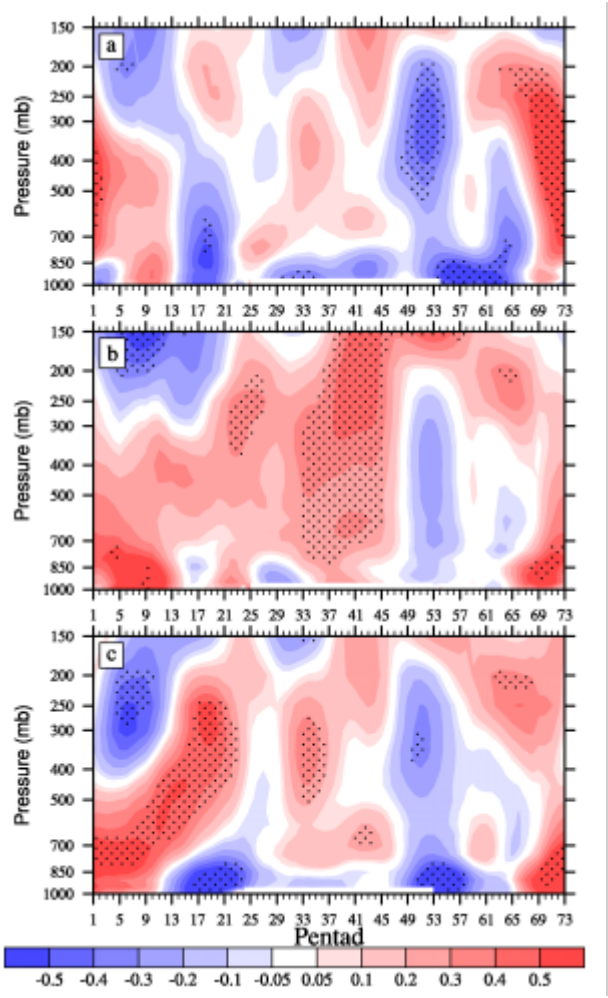

2015JD024574-f10-z-.tif

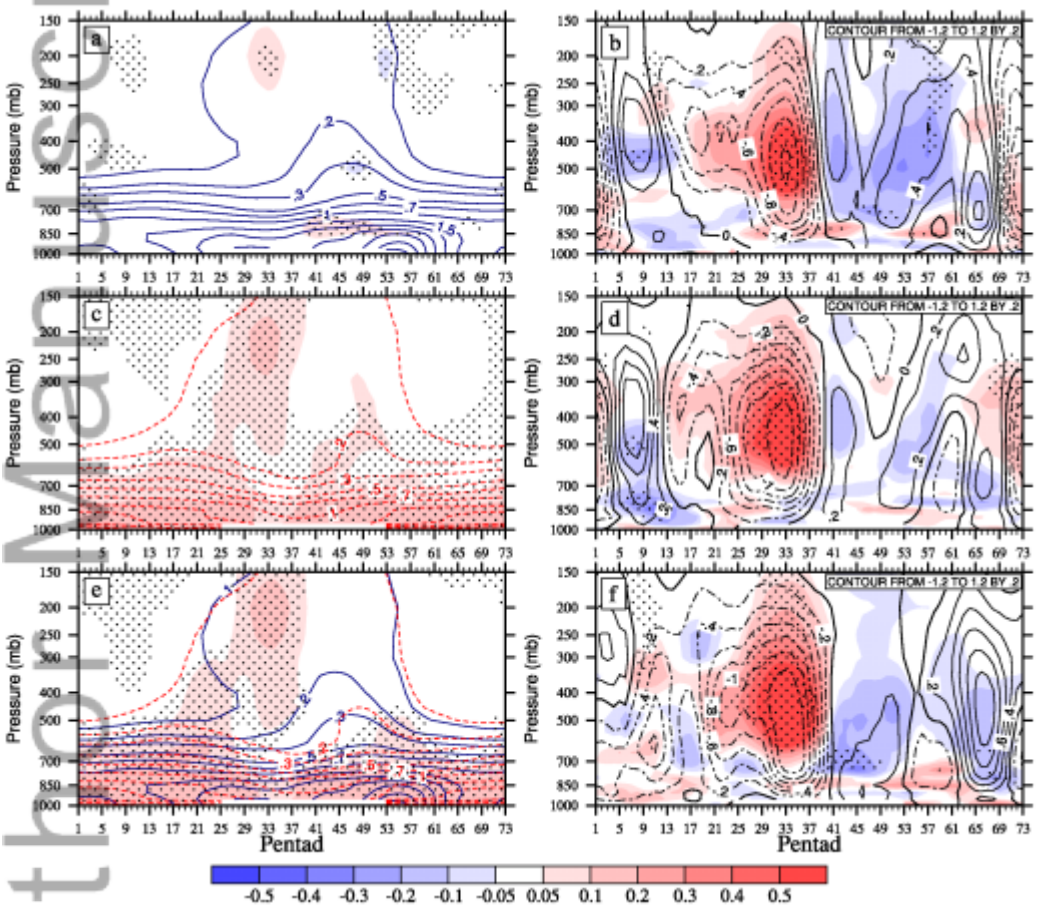

2015JD024574-f11-z-.tif